Online Appendix for "The Innovation Long-Run Risk Component" (2026)

Fabio Franceschini[a,*]

[a] *Department of Economics, University of Bologna, Piazza Scaravilli 2, Bologna, 40126, Italy*

Contents

Appendix A Theoretical Derivations **2**
Appendix A.1 Key Linearized Conditions 2
Appendix A.2 Balanced Growth Path 3
Appendix A.3 Short-Run System in Observables 4
Appendix A.4 Effective R&D Levels 5

Appendix B Empirical Macroeconomic Details **6**
Appendix B.1 Macroeconomic Data 6
Appendix B.2 An Estimator of Net Effective R&D 9
Appendix B.3 Interpretation of Local Projection Coefficients 12

Appendix C Empirical Financial Details **12**
Appendix C.1 Financial Data 12
Appendix C.2 Risk Premia Estimation with Omitted Factors 20
Appendix C.3 Cash-Flow-Based Asset Pricing 20

Appendix D Additional Results **21**
Appendix D.1 Related Measures 21
Appendix D.2 Three-Shock Structural System 23
Appendix D.3 Other Tables 27
Appendix D.4 Other Figures 27

References **31**

*Corresponding author.
Email address: franceschini-f@pm.me (Fabio Franceschini)
URL: franceschini-f.github.io (Fabio Franceschini)

Appendix A. Theoretical Derivations

Appendix A.1. Key Linearized Conditions

Taking logarithms and first differences of (7) yields

$$\Delta \ln Z_t = \theta \cdot \Delta \ln I_t + \xi \cdot \Delta \ln Q_t + \Delta a_t \,. \tag{A.1}$$

Dividing both sides of (8) by I_t and taking logarithms gives the growth rate of ideas:

$$\Delta \ln I_{t+1} = \ln \left\{ 1 - \phi + \chi \cdot S_t^{\eta} I_t^{-(1-\psi)} Q_t^{-1} \right\} , \tag{A.2}$$

which, for small $\Delta \ln I_{t+1}$, is well approximated by

$$\Delta \ln I_{t+1} \approx -\phi + \chi \cdot S_t^{\eta} I_t^{-(1-\psi)} Q_t^{-1} \,. \tag{A.3}$$

The approximation sharpens as the time step shortens, since ϕ and the per-period flow of new ideas both scale down with the period length, driving $\Delta \ln I_{t+1}$ to zero in the continuous-time limit.

Let $X_t = S_t^{\eta} I_t^{-(1-\psi)} Q_t^{-1}$. If $\Delta \ln Z_t$, $\Delta \ln Q_t$ and Δa_t are stationary,[1] then a literal interpretation of (A.1) forces $\Delta \ln I_{t+1}$, and hence X_t, to be stationary too. Taylor-expanding X_t around $\ln \mathbb{E}[X_t]$ gives

$$X_t = \exp\{\ln[X_t]\} \approx \exp\{\ln \mathbb{E}[X_t]\} + \exp\{\ln \mathbb{E}[X_t]\} (\ln X_t - \ln \mathbb{E}[X_t]) \tag{A.4}$$

$$= \mathbb{E}[X_t] (1 - \ln \mathbb{E}[X_t]) + \mathbb{E}[X_t] \cdot \ln X_t \,, \tag{A.5}$$

and substituting back yields

$$\Delta \ln I_{t+1} \approx -\phi + \chi \cdot \mathbb{E}[X_t] (1 - \ln \mathbb{E}[X_t]) + \chi \cdot \mathbb{E}[X_t] \cdot \ln X_t \tag{A.6}$$

$$= \gamma_{0,I} + \gamma_{1,I} \left[\ln S_t - \frac{1-\psi}{\eta} \ln I_t - \frac{1}{\eta} \ln Q_t \right] . \tag{A.7}$$

Plugging this into (A.1) and denoting effective R&D s_t as in (10),

$$\Delta \ln Z_{t+1} = \gamma_{0,Z} + \gamma_1 \cdot s_t + \xi \cdot \Delta \ln Q_{t+1} + \Delta a_{t+1} \,. \tag{A.8}$$

Decomposing effective R&D into mean and deviation $s_t = \bar{s} + \tilde{s}_t$, and substituting into its definition $\ln I_t = \frac{1}{\theta} \ln Z_t - \frac{\xi}{\theta} \ln Q_t - \frac{1}{\theta} a_t$ from (7) and $\ln Q_t$ from (15),

$$\bar{s} + \tilde{s}_t = \ln S_t - \overbrace{\frac{1-\psi}{\eta\theta}}^{\alpha_Z} \left(\ln Z_t - a_t \right) - \overbrace{\left(\frac{1}{\eta} - \frac{(1-\psi)\xi}{\eta\theta} \right)}^{\alpha_L/\omega} \left(\omega \ln L_t + \pi a_t \right) \tag{A.9}$$

$$= \bar{s} + \hat{s}_t + \left(\alpha_Z + \alpha_L \frac{\pi}{\omega} \right) a_t \,, \tag{A.10}$$

delivers, with a slight abuse of notation ($\gamma_{0,Z}$ now absorbs additional constants),

$$\Delta \ln Z_{t+1} = \gamma_{0,Z} + \gamma_1 \cdot \hat{s}_t + \xi \cdot \Delta \ln Q_{t+1} + \Delta a_{t+1} + \gamma_{2,Z} \cdot a_t \,. \tag{A.11}$$

[1] Stationarity of $\Delta \ln Z_t$ enjoys broad empirical support, while stationarity of $\Delta \ln Q_t$ and Δa_t is standard in the theoretical literature; the observable component of $\Delta \ln Q_t$ used here, $\Delta \ln L_t$, is itself clearly stationary in the data.

Appendix A.2. Balanced Growth Path

In addition to conditions (6), (7) and (8) from Section 2, and condition (15) from Section 3, consider the economy's resource constraint

$$Y_t = C_t + S_t\,, \tag{A.12}$$

where C_t is consumption, and a constant labor-force growth rate $\Delta \ln L_t = \mu_L > 0$. Combining (6), (7) and (15) yields

$$g_Y = \theta g_I + (1 + \xi\omega)\mu_L\,, \tag{A.13}$$

where g_j denotes the unconditional expected growth rate of $j \in \{Y, Z, L, I, Q\}$.

A balanced growth path (BGP) in the *fully endogenous* regime requires the joint restriction

$$\frac{1-\psi}{\theta} = \eta = \frac{\omega}{1+\omega\xi}\,. \tag{A.14}$$

Under this restriction, the R&D share $\breve{s}_t$, defined by

$$S_t = e^{\breve{s}_t} Y_t\,, \tag{A.15}$$

can be stationary, implying $g_S = g_Y$, and delivers stationary growth rates with

$$g_I = -\phi + \chi \cdot \breve{s}\,, \tag{A.16}$$

where $\breve{s} = \mathbb{E}[\breve{s}_t]$. Two remarks are in order. First, under these restrictions the R&D share of output coincides with the effective R&D variable. Second, most empirical evidence does not support stationarity of the R&D share of GDP, although caveats apply when mapping this theoretical condition to the data.

A BGP in the *semi-endogenous* regime requires only

$$\begin{cases} \omega < \frac{\eta}{1-\xi\eta} & \text{if } \psi < 1 - \eta\theta\,, \\ \omega > \frac{\eta}{1-\xi\eta} & \text{if } \psi > 1 - \eta\theta\,. \end{cases} \tag{A.17}$$

Under these conditions, a stationary R&D share $\breve{s}_t$ delivers stationary growth rates with

$$g_I = \frac{\eta(1+\omega\xi) - \omega}{1 - \psi - \eta\theta}\,\mu_L\,. \tag{A.18}$$

Notably, stationary growth rates and effective R&D are also compatible with an R&D share of output that is integrated of order one. In that case, $g_S = \mu_S + g_Y$ for some constant $\mu_S = \mathbb{E}[\Delta\breve{s}_t]$, and the steady-state idea growth rate becomes

$$g_I = \frac{\eta}{1 - \psi - \eta\theta}\,\mu_S + \frac{\eta(1+\omega\xi) - \omega}{1 - \psi - \eta\theta}\,\mu_L\,. \tag{A.19}$$

Kung and Schmid (2015) satisfies the restriction for a fully endogenous growth regime BGP by setting $\xi = \mu_L = 0$, $\theta = 1$, and $\eta = 1 - \psi$.

Finally, given the definitions of α_Z and α_L, the fully endogenous BGP restriction $\frac{1-\psi}{\theta} = \eta$ implies

$$\alpha_Z = 1\,, \tag{A.20}$$

while positive spillovers from the past stock of ideas, $\psi > 0$, imply

$$\theta\eta < \frac{1}{\alpha_Z} \qquad \text{and} \qquad \theta < \frac{\alpha_L}{\alpha_Z} + \xi\omega\,. \tag{A.21}$$

Appendix A.3. Short-Run System in Observables

As a preliminary step, substitute

$$\tilde{s}_t = \hat{s}_t + \left(\alpha_Z + \alpha_L \cdot \frac{\pi}{\omega}\right) a_t \tag{A.22}$$

from (17) into

$$\Delta a_{t+1} = \beta_{a,s}\tilde{s}_t + (\rho_a - 1)a_t + \beta_{a,L}\widetilde{\Delta \ln L}_t + \delta_{a,a}\varepsilon^a_{t+1} \tag{A.23}$$

from (18b), which yields

$$\Delta a_{t+1} = \beta_{a,s}\hat{s}_t + \left(\rho_a - 1 + \beta_{a,s}\left(\alpha_Z + \alpha_L \cdot \frac{\pi}{\omega}\right)\right) a_t + \beta_{a,L}\widetilde{\Delta \ln L}_t + \delta_{a,a}\varepsilon^a_{t+1}\,. \tag{A.24}$$

Next, combine the definition of productivity growth with the short-run structural relations in (18). First, substituting (A.22) into (18c) gives

$$\widetilde{\Delta \ln L}_{t+1} = \beta_{L,s}\hat{s}_t + \beta_{L,s}\left[\left(\alpha_Z + \alpha_L \cdot \frac{\pi}{\omega}\right) + \beta_{L,a}\right] a_t + \rho_L\widetilde{\Delta \ln L}_t + \delta_{L,a}\varepsilon^a_{t+1}\,. \tag{A.25}$$

Second, substituting $\Delta \ln Q_{t+1} = \omega\Delta \ln L_{t+1} + \pi\Delta a_{t+1}$ from (15) into (9) gives

$$\Delta \ln Z_{t+1} \approx \gamma_0 + \gamma_1 \cdot \tilde{s}_t + \xi\omega \cdot \Delta \ln L_{t+1} + (1 + \xi\pi)\Delta a_{t+1}\,, \tag{A.26}$$

and substituting Δa_{t+1} from (A.23) and $\widetilde{\Delta \ln L}_{t+1}$ from (18c) yields

$$\begin{aligned}\widetilde{\Delta \ln Z}_{t+1} \approx\ & \left(\gamma_1 + \xi\omega\beta_{L,s} + (1 + \xi\pi)\beta_{a,s}\right)\tilde{s}_t \\ & + \left[\xi\omega\beta_{L,a} + (1 + \xi\pi)(\rho_a - 1)\right]a_t + \left[\xi\omega\rho_L + (1 + \xi\pi)\beta_{a,L}\right]\widetilde{\Delta \ln L}_t \\ & + \left[\xi\omega\delta_{L,a} + (1 + \xi\pi)\delta_{a,a}\right]\varepsilon^a_{t+1}\,.\end{aligned} \tag{A.27}$$

Further substituting (A.22) gives

$$\begin{aligned}\widetilde{\Delta \ln Z}_{t+1} \approx\ & \left(\gamma_1 + \xi\omega\beta_{L,s} + (1 + \xi\pi)\beta_{a,s}\right)\hat{s}_t \\ & + \left[\left(\gamma_1 + \xi\omega\beta_{L,s} + (1 + \xi\pi)\beta_{a,s}\right)\left(\alpha_Z + \alpha_L \cdot \frac{\pi}{\omega}\right) + \xi\omega\beta_{L,a} + (1 + \xi\pi)(\rho_a - 1)\right]a_t \\ & + \left[\xi\omega\rho_L + (1 + \xi\pi)\beta_{a,L}\right]\widetilde{\Delta \ln L}_t \\ & + \left[\xi\omega\delta_{L,a} + (1 + \xi\pi)\delta_{a,a}\right]\varepsilon^a_{t+1}\,.\end{aligned} \tag{A.28}$$

Third, substituting (A.22) into (18a) gives

$$\begin{aligned}\hat{s}_{t+1} + \left(\alpha_Z + \alpha_L \cdot \frac{\pi}{\omega}\right)\Delta a_{t+1} = \rho_s\hat{s}_t + \left[(\rho_s - 1)\left(\alpha_Z + \alpha_L \cdot \frac{\pi}{\omega}\right) + \beta_{s,a}\right]a_t + \beta_{s,L}\widetilde{\Delta \ln L}_t \\ + \delta_{s,a}\varepsilon^a_{t+1} + \delta_{s,s}\varepsilon^s_{t+1}\,,\end{aligned} \tag{A.29}$$

and combining with (A.24) yields

$$\begin{aligned}\hat{s}_{t+1} =\ & \left(\rho_s - \left(\alpha_Z + \alpha_L \cdot \frac{\pi}{\omega}\right)\beta_{a,s}\right)\hat{s}_t \\ & + \left[(\rho_s - 1)\left(\alpha_Z + \alpha_L \cdot \frac{\pi}{\omega}\right) + \beta_{s,a} - \left(\alpha_Z + \alpha_L \cdot \frac{\pi}{\omega}\right)\left(\rho_a - 1 + \beta_{a,s}\left(\alpha_Z + \alpha_L \cdot \frac{\pi}{\omega}\right)\right)\right]a_t \\ & + \left(\beta_{s,L} - \left(\alpha_Z + \alpha_L \cdot \frac{\pi}{\omega}\right)\beta_{a,L}\right)\widetilde{\Delta \ln L}_t \\ & + \left(\delta_{s,a} - \left(\alpha_Z + \alpha_L \cdot \frac{\pi}{\omega}\right)\delta_{a,a}\right)\varepsilon^a_{t+1} + (\delta_{s,s})\,\varepsilon^s_{t+1}\,.\end{aligned} \tag{A.30}$$

Fourth, substituting (A.22) into (18b) gives

$$a_{t+1} = \beta_{a,s}\hat{s}_t + \left[\rho_a + \beta_{a,s}\left(\alpha_Z + \alpha_L \cdot \frac{\pi}{\omega}\right)\right] a_t + \beta_{a,L}\widetilde{\Delta \ln L}_t + \delta_{a,a}\varepsilon^a_{t+1}\,. \tag{A.31}$$

Finally, the system (18) can be expressed as

$$\begin{bmatrix} \boldsymbol{x}_{t+1} \\ \boldsymbol{y}_{t+1} \end{bmatrix} = \begin{pmatrix} B_{x,x} & B_{x,y} \\ B_{y,x} & B_{y,y} \end{pmatrix} \begin{bmatrix} \boldsymbol{x}_t \\ \boldsymbol{y}_t \end{bmatrix} + \begin{pmatrix} D_x \\ D_y \end{pmatrix} \boldsymbol{\varepsilon}_{t+1}\,, \tag{A.32}$$

where $\boldsymbol{x}_t$ is $\left[\hat{s}_t,\ \widetilde{\Delta \ln Z}_t\right]'$, $\boldsymbol{y}_t$ is $\left[\widetilde{\Delta \ln L}_t, a_t\right]'$, and $\boldsymbol{\varepsilon}_{t+1}$ is $[\varepsilon^s_{t+1}, \varepsilon^a_{t+1}]'$; the blocks $B_{i,j}$ and D_i for $i, j \in \{x, y\}$ are implicitly defined by (A.30), (A.28), (A.25), and (A.31). Equivalently,

$$\boldsymbol{x}_{t+1} = B_{x,x}\boldsymbol{x}_t + B_{x,y}\boldsymbol{y}_t + D_x\boldsymbol{\varepsilon}_{t+1} \tag{A.33}$$

$$\boldsymbol{y}_{t+1} = B_{y,x}\boldsymbol{x}_t + B_{y,y}\boldsymbol{y}_t + D_y\boldsymbol{\varepsilon}_{t+1}\,. \tag{A.34}$$

Substituting the lag of (A.34) into (A.33) gives

$$\boldsymbol{x}_{t+1} = B_{x,x}\boldsymbol{x}_t + B_{x,y}B_{y,x}\boldsymbol{x}_{t-1} + B_{y,y}(B_{x,y}\boldsymbol{y}_{t-1}) + D_x\boldsymbol{\varepsilon}_{t+1} + B_{x,y}D_y\boldsymbol{\varepsilon}_t \tag{A.35}$$

and the lag of (A.33) provides

$$B_{x,y}\boldsymbol{y}_{t-1} = \boldsymbol{x}_t - B_{x,x}\boldsymbol{x}_{t-1} - D_x\boldsymbol{\varepsilon}_t\,, \tag{A.36}$$

yielding

$$\begin{aligned} \boldsymbol{x}_{t+1} = (B_{x,x} + B_{y,y})\boldsymbol{x}_t + (B_{x,y}B_{y,x} - B_{y,y}B_{x,x})\boldsymbol{x}_{t-1} \\ + D_x\boldsymbol{\varepsilon}_{t+1} + (B_{x,y}D_y - B_{y,y}D_x)\boldsymbol{\varepsilon}_t\,. \end{aligned} \tag{A.37}$$

Expanding and relabelling gives (19).

Appendix A.4. Effective R&D Levels

Maintaining stationarity assumptions, (9) and (15) give

$$\widetilde{\Delta \ln Z}_{t+1} = \gamma_1 \cdot \tilde{s}_t + (\xi\omega)\widetilde{\Delta \ln L}_{t+1} + (1 + \xi\pi)\Delta a_{t+1}\,, \tag{A.38}$$

while the definition of gross effective R&D in (17) gives

$$\Delta a_t = \frac{\Delta\tilde{s}_t - \Delta\hat{s}_t}{\alpha_Z + \alpha_L\frac{\pi}{\omega}}\,. \tag{A.39}$$

Substituting the latter into the former yields

$$\widetilde{\Delta \ln Z}_{t+1} = \gamma_1 \cdot \tilde{s}_t + (\xi\omega)\widetilde{\Delta \ln L}_{t+1} + (1 + \xi\pi)\left(\frac{\Delta\tilde{s}_{t+1} - \Delta\hat{s}_{t+1}}{\alpha_Z + \alpha_L\frac{\pi}{\omega}}\right)\,. \tag{A.40}$$

Expanding the R&D differences and rearranging gives

$$\tilde{s}_{t+1} = \left(\frac{\alpha_Z + \alpha_L\frac{\pi}{\omega}}{1 + \xi\pi}\right)\left[\widetilde{\Delta \ln Z}_{t+1} - (\xi\omega)\widetilde{\Delta \ln L}_{t+1}\right] + \Delta\hat{s}_{t+1} + \left(1 - \gamma_1\left(\frac{\alpha_Z + \alpha_L\frac{\pi}{\omega}}{1 + \xi\pi}\right)\right)\tilde{s}_t\,. \tag{A.41}$$

Recursively substituting $\tilde{s}_t$ and collecting terms returns (20).

Appendix B. Empirical Macroeconomic Details

Appendix B.1. Macroeconomic Data

This section presents the macroeconomic data used in the paper, documenting each series together with its source, identifier, and any transformations applied.

The baseline real R&D series is constructed by deflating the nominal R&D series (`Y006RC1Q027SBEA`) with the corresponding price deflator (`Y006RG3Q086SBEA`), yielding a series in chained 2017 dollars, while the associated total series is `Y694RX1Q020SBEA`; all are produced by the Bureau of Economic Analysis (BEA) and retrieved through the Federal Reserve Economic Data (FRED) database. The TFP data are provided online by the author of Fernald (2012), including the utilization adjustment as well as changes in capital excluding R&D. Labor input is based on the series `CE16OV` and `LNS12035019`, both reported at monthly frequency by the Bureau of Labor Statistics (BLS), obtained through FRED, and aggregated by taking the last observation each quarter. Consumption is measured as real total personal consumption expenditures per capita in chained 2017 US dollars (`A794RX0Q048SBEA`), provided by the BEA through FRED, spanning 1948Q1–2025Q2.

The macroeconomic factors consist of two distinct sets, previously employed to forecast TFP growth in Ai et al. (2018): (1) nine identified factors, extending those used in Bansal and Shaliastovich (2013); and (2) nine non-identified factors taken directly from Ludvigson and Ng (2009), referred to with the shorthands "BS" and "LN", respectively. The BS set originally comprised the US Cyclically Adjusted Price-to-Earnings (CAPE) ratio, the 3-month Treasury-bill yield, and the 3- and 5-year Treasury bond yields, to which Ai et al. (2018) added the integrated daily volatility of the US stock market; the present work further incorporates the 10-year Treasury bond yield, real US corporate profits, and real US nonfinancial corporate liquid assets, in order to better capture macroeconomic dynamics at longer horizons as well as aspects related to financing conditions, profitability, and product proliferation – all known to influence productivity and R&D decisions. The underlying BS data are drawn from several sources: the CAPE ratio is from R. Shiller's website; the bill and bond yields are taken from Finaeon up to the first availability of `DGS3MO`, `DGS3`, `DGS5`, and `DGS10` on FRED, after which the FRED series are used; daily stock market data are from CRSP; and real corporate profits and real nonfinancial corporate liquid assets are constructed from `CPROFIT` and `BOGZ1FL104001005Q` (FRED), each deflated by the GDP deflator `GDPDEF` (FRED). The LN set, by contrast, is formed from the principal components of a broad array of macroeconomic and financial variables, is publicly available on S. Ludvigson's website, and is reported at monthly frequency, aggregated to quarterly averages. All BS variables appear to exhibit unit-root behaviour, whereas there is only weak evidence of non-stationarity among the LN factors; accordingly, the LN factors are used in levels, while the BS factors enter in first differences to mitigate the risk of spurious regression.

Figure B.1 plots all series, while Tables B.1, B.2, and B.3 report descriptive statistics together with stationarity diagnostics for the effective-R&D data, the BS factors, and the LN factors, respectively.



Figure B.1: Raw macroeconomic data, displayed in three stacked panels. The top panel ($\hat{s}$) collects the series used to estimate effective R&D, while the middle and bottom panels report the *BS* and *LN* factor sets, respectively. Consistent with the transformations adopted in the analysis, the $\hat{s}$ series and the LN factors are shown in levels, whereas the BS factors are shown in first differences.

Table B.1: Descriptive statistics for the effective-R&D data. *N. Obs.* is the number of observations; *tt* and tt^2 are the coefficients on a linear and quadratic time trend (HAC standard errors); *AR(1)* is the slope from an AR(1) fit; and *ADF* and *KPSS* are the Augmented Dickey–Fuller and KPSS tests, with null hypotheses of a unit root and of stationarity, respectively, computed in levels.

	Priv. R&D	Tot. R&D	Raw TFP	Adj. TFP	Tot. Empl.	N.F. Empl.
tt	0.017***	0.019**	0.018***	0.018***	0.018***	0.017***
tt^2	−0.000	−0.000	−0.000***	−0.000	−0.000***	−0.000***
AR(1)	1.000***	1.000***	1.000***	1.000***	1.000***	1.000***
ADF	−1.482	−2.027**	−2.346**	−2.891***	−1.353	−0.948
KPSS	2.004***	1.924***	1.976***	1.978***	2.001***	2.011***
N. Obs.	314	314	314	314	310	310

$^{***}p < 0.01$, $^{**}p < 0.05$, $^{*}p < 0.1$

Table B.2: Descriptive statistics for the BS factors. Statistics are defined as in Table B.1, but the *ADF* and *KPSS* tests are computed on the first-differenced series used in the analysis.

	CAPE	10Y yield	3M yield	3Y yield	5Y yield	Int. Vol	Corp. Profits	N.F. Liq. Assets
tt	-0.001	-0.004^{*}	-0.003	-0.004^{*}	-0.004^{*}	0.002	0.002	0.005^{*}
tt^2	0.000	0.000	0.000	0.000	0.000	-0.000	-0.000	-0.000
AR(1)	-0.334^{***}	-0.053	-0.187^{***}	-0.117^{*}	-0.102^{*}	-0.297^{***}	0.031	0.068
ADF	-13.638^{***}	-11.188^{***}	-13.206^{***}	-11.844^{***}	-11.734^{***}	-15.514^{***}	-10.569^{***}	-10.688^{***}
KPSS	0.078^{*}	0.184^{*}	0.099^{*}	0.144^{*}	0.170^{*}	0.259^{*}	0.052^{*}	0.097^{*}
N. Obs.	270	270	270	270	270	270	270	269

$^{***}p < 0.01$, $^{**}p < 0.05$, $^{*}p < 0.1$

Table B.3: Descriptive statistics for the LN factors. Statistics are defined as in Table B.1 and computed in levels.

	f1	f2	f3	f4	f5	f6	f7	f8	f9
tt	0.005	0.005	0.002	-0.004	-0.001	0.006	-0.001	0.017^{***}	0.003
tt^2	-0.000	-0.000	0.000	0.000	-0.000	-0.000	0.000	-0.000^{***}	-0.000
AR(1)	0.725^{***}	0.360^{***}	0.749^{***}	0.426^{***}	0.703^{***}	0.620^{***}	0.138^{**}	0.513^{***}	0.329^{***}
ADF	-6.467^{***}	-7.252^{***}	-4.577^{***}	-6.929^{***}	-4.911^{***}	-5.758^{***}	-10.204^{***}	-7.415^{***}	-9.526^{***}
KPSS	0.324^{*}	0.514^{**}	0.525^{**}	0.373^{*}	0.224^{*}	0.278^{*}	0.190^{*}	0.603^{**}	0.062^{*}
N. Obs.	262	262	262	262	262	262	262	262	262

$^{***}p < 0.01$, $^{**}p < 0.05$, $^{*}p < 0.1$

Appendix B.2. An Estimator of Net Effective R&D

The error of the recovery estimator $\hat{\tilde{s}}_t$ relative to the true $\tilde{s}_t$ decomposes as

$$\hat{\tilde{s}}_t - \tilde{s}_t = (\hat{\tilde{s}}_t - \tilde{\tilde{s}}_t) + (\tilde{\tilde{s}}_t - \tilde{s}_t)\,, \tag{B.1}$$

where $\tilde{\tilde{s}}_t = \hat{\tilde{s}}_t + \hat{\kappa}_s^t\,\tilde{s}_0$ is an infeasible companion that retains the initial-condition term. Throughout, $X = \{\Delta \ln Z_t, \Delta \ln L_t\}_{t=1}^T$ denotes the regressors sample, and $\hat{\boldsymbol{b}} = (\hat{b}_s, \hat{b}_Z, \hat{b}_L)$ the vector of parameter estimates entering the recovery. The three quantities in (B.1) can then be written as $\hat{\tilde{s}}_t = g_t(\hat{\boldsymbol{b}})$, $\tilde{\tilde{s}}_t = g_t(\hat{\boldsymbol{b}}) + \hat{\kappa}_s^t\tilde{s}_0$, and $\tilde{s}_t = g_t(\boldsymbol{b}) + \kappa_s^t\tilde{s}_0$.

The first summand, $-\hat{\kappa}_s^t\tilde{s}_0$, shrinks as t grows, since $\hat{\kappa}_s^t$ decays geometrically (provided $\hat{\kappa}_s \in (0,1)$); to make it vanish for every t that the estimator retains, the minimum retained t must grow with the sample size. This is implemented by retaining only estimates at $t \geq \tau$, where the cutoff is

$$\tau(T, \hat{\kappa}_s, \gamma) = \left\lceil \frac{\gamma \log T}{\log(1/\hat{\kappa}_s)} \right\rceil\,, \tag{B.2}$$

chosen so that $\hat{\kappa}_s^\tau = T^{-\gamma}$, which makes the rule adapt to the persistence of $\tilde{s}_t$: the smaller $\hat{\kappa}_s$, the shorter the burn-in. With this cutoff in place, at every retained t the first summand vanishes in probability at rate $T^{-\gamma}$ as $T \to \infty$, for any $\gamma > 0$. Moreover, since the cutoff grows only logarithmically with T, $\tau/T \to 0$ and the number of retained estimates is asymptotically of the same size as T. The second summand, $\tilde{\tilde{s}}_t - \tilde{s}_t$, is a smooth (continuous and differentiable) function of the parameter estimates. By the continuous mapping theorem, the consistency of those estimates carries over, so $\tilde{\tilde{s}}_t - \tilde{s}_t \xrightarrow{p} 0$ as $\hat{\boldsymbol{b}} \xrightarrow{p} \boldsymbol{b}$. Both summands vanishing in probability delivers $\hat{\tilde{s}}_t \xrightarrow{p} \tilde{s}_t$.

The variance of $\hat{\tilde{s}}_t - \tilde{s}_t$ decomposes, via the law of total variance conditional on $\hat{\boldsymbol{b}}$, into a parameter-sampling component $V_{b,t}$ and an omission component $V_{o,t}$:

$$\operatorname{Var}\left(\hat{\tilde{s}}_t - \tilde{s}_t \,\middle|\, X\right) = V_{b,t} + V_{o,t}\,. \tag{B.3}$$

The first term is

$$V_{b,t} = \operatorname{Var}\left(\mathbb{E}\big[\hat{\tilde{s}}_t - \tilde{s}_t \big| \hat{\boldsymbol{b}}, X\big] \,\middle|\, X\right) = \operatorname{Var}\left(g_t(\hat{\boldsymbol{b}}) - g_t(\boldsymbol{b}) \,\middle|\, X\right)\,, \tag{B.4}$$

since $\mathbb{E}[\tilde{s}_0 \mid \hat{\boldsymbol{b}}, X] = \mathbb{E}[\tilde{s}_0] = 0$ under independence of $\tilde{s}_0$ from $\hat{\boldsymbol{b}}$ and X. The second is

$$V_{o,t} = \mathbb{E}\left[\operatorname{Var}\left(\hat{\tilde{s}}_t - \tilde{s}_t \,\middle|\, \hat{\boldsymbol{b}}, X\right) \,\middle|\, X\right] = \kappa_s^{2t}\operatorname{Var}(\tilde{s}_0)\,, \tag{B.5}$$

since, conditional on $\hat{\boldsymbol{b}}$ and X, the only random quantity is $\tilde{s}_0$, with $\operatorname{Var}(\tilde{s}_0 \mid \hat{\boldsymbol{b}}, X) = \operatorname{Var}(\tilde{s}_0)$ by the same argument.

The parameter-sampling component $V_{b,t}$ captures the variance of $\hat{\tilde{s}}_t - \tilde{s}_t$ induced by the sampling distribution of $\hat{\boldsymbol{b}}$. Since $g_t(\boldsymbol{b})$ is smooth in $\boldsymbol{b}$, the delta method gives

$$\widehat{V}_{b,t} = \nabla g_t(\hat{\boldsymbol{b}})'\,\widehat{\operatorname{Var}}(\hat{\boldsymbol{b}})\,\nabla g_t(\hat{\boldsymbol{b}})\,, \tag{B.6}$$

where $\widehat{\operatorname{Var}}(\hat{\boldsymbol{b}})$ is the estimated covariance matrix of the parameter estimates and $\nabla g_t(\hat{\boldsymbol{b}})$ is the gradient of g_t, evaluated at $\hat{\boldsymbol{b}}$. Substituting the residual $\Delta e_t = \widetilde{\Delta \ln S_t} - b_Z\widetilde{\Delta \ln Z_t} - b_L\widetilde{\Delta \ln L_t}$ from (22) into (23),

$$g_t(\boldsymbol{b}) = \sum_{j=0}^{t-1}(1 - b_s \cdot b_Z)^j \left(\widetilde{\Delta \ln S_{t-j}} - \widetilde{\Delta \ln L_{t-j}}\right)\,, \tag{B.7}$$

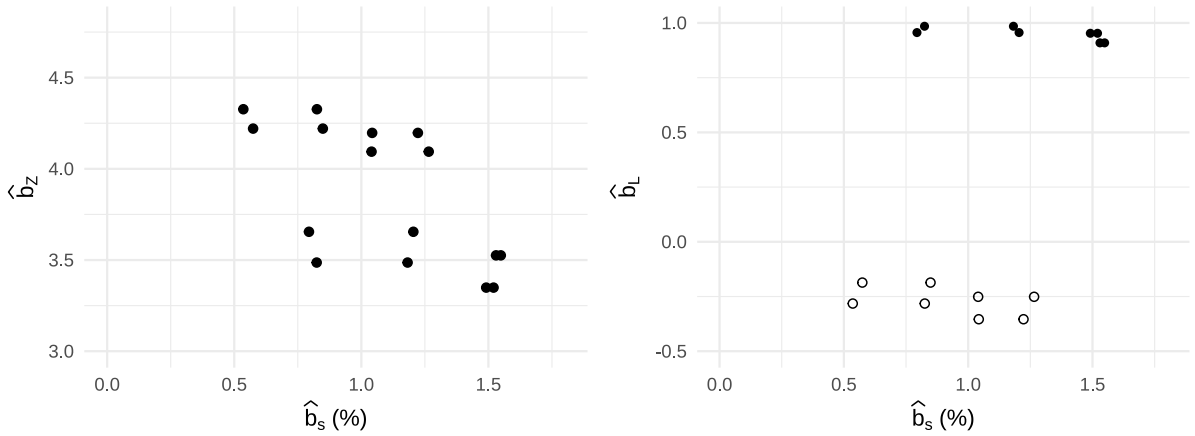


Figure B.2: Values of $\hat{b}_s$, $\hat{b}_Z$ (left panel), and $\hat{b}_L$ (right panel) across the 16 cointegration specifications considered in this work. Hollow dots indicate specifications where the coefficient estimate is not significant at the 10% level. A linear regression of $\hat{b}_Z$ on $\hat{b}_s$ yields a slope of -0.7 with a HC t-statistic < -4. For $\hat{b}_L$, the slope is -0.06 with -1.69 HC t-statistic.

so its gradient is

$$\nabla g_t(\boldsymbol{b}) = \begin{bmatrix} -b_Z \sum_{j=0}^{t-1} \left\{ j \cdot \kappa_s^{j-1} \left(\widetilde{\Delta \ln S}_{t-j} - \widetilde{\Delta \ln L}_{t-j} \right) \right\} \\ -b_s \sum_{j=0}^{t-1} \left\{ j \cdot \kappa_s^{j-1} \left(\widetilde{\Delta \ln S}_{t-j} - \widetilde{\Delta \ln L}_{t-j} \right) \right\} \\ 0 \end{bmatrix} . \tag{B.8}$$

The sampling covariances of $\hat{b}_s$ with the cointegration estimates $\hat{b}_Z$ and $\hat{b}_L$ are unknown, but the point estimates are negatively correlated across the 16 specifications in this study (Figure B.2), suggesting negative sampling covariances as well. Setting them to zero is therefore conservative, yielding a heuristic upper bound on $V_{b,t}$:

$$\widehat{\mathrm{Var}}(\hat{\boldsymbol{b}}) = \begin{bmatrix} \hat{\sigma}^2_{b_s} & 0 & 0 \\ 0 & \hat{\sigma}^2_{b_Z} & \hat{\sigma}_{b_Z,b_L} \\ 0 & \hat{\sigma}_{b_Z,b_L} & \hat{\sigma}^2_{b_L} \end{bmatrix} . \tag{B.9}$$

Since $\partial g_t / \partial b_L = 0$, the third row and column are annihilated by the gradient: neither $\hat{\sigma}^2_{b_L}$ nor $\hat{\sigma}_{b_Z,b_L}$ enters $\widehat{V}_{b,t}$, which depends only on the (b_s, b_Z) block.

The omission component $V_{o,t}$ measures the uncertainty arising from the unobservability of the initial condition $\tilde{s}_0$, and it is estimated by plug-in:

$$\widehat{V}_{o,t} = \hat{\kappa}_s^{2t} \cdot \hat{\sigma}^2_{\tilde{s}} , \tag{B.10}$$

where $\hat{\sigma}^2_{\tilde{s}} = \frac{1}{T-\tau+1} \sum_{t=\tau}^{T} \hat{\tilde{s}}^2_t$. Under stationarity of $\tilde{s}_t$, the continuous mapping theorem delivers consistency of $\hat{\kappa}_s$ for κ_s and of $\hat{\sigma}^2_{\tilde{s}}$ for $\mathrm{Var}(\tilde{s}_0)$.

Figure B.3 shows the information criteria used to select the specifications reported in Table 2. The $\hat{\kappa}_s^t$ implied by these estimates is shown in Figure B.4, for the main specifications. $\hat{\kappa}_s^t$ declines steadily but approaches zero only in the second half of the sample. At $\gamma = 0.35$, the cutoffs τ correspond to $\hat{\kappa}_s^\tau \approx 0.13$.

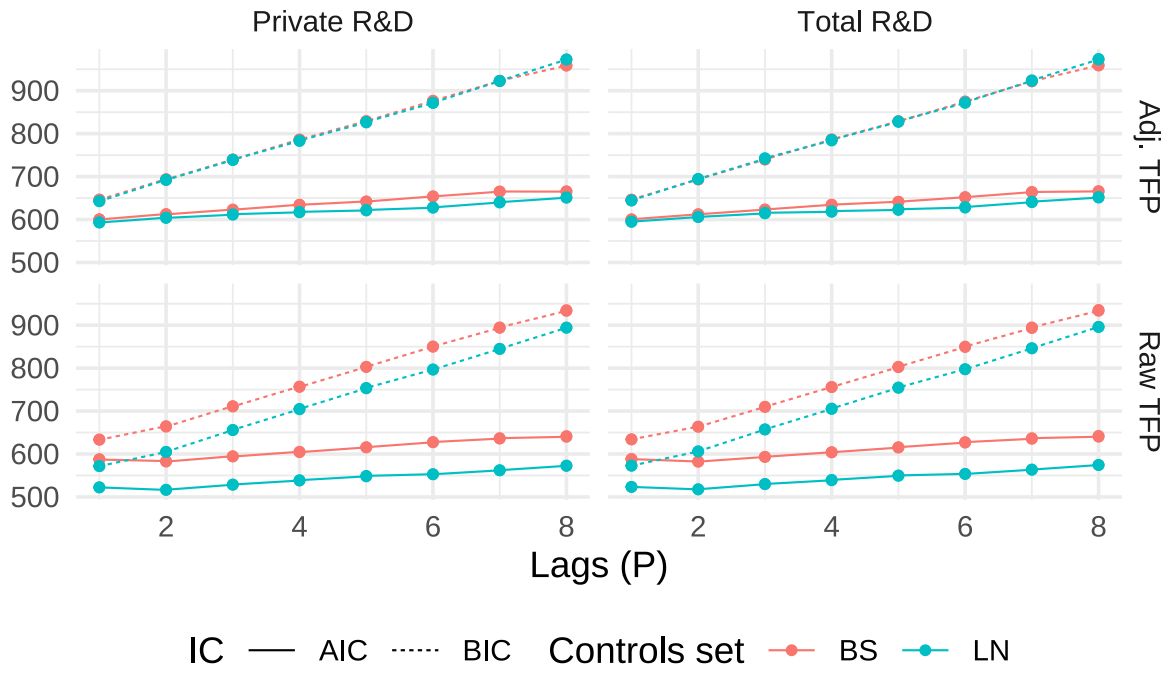


Figure B.3: Information criteria used to select the specifications in Table 2, computed on the largest sample common to all specifications with baseline employment. Results using nonfarm employment are visually indistinguishable.

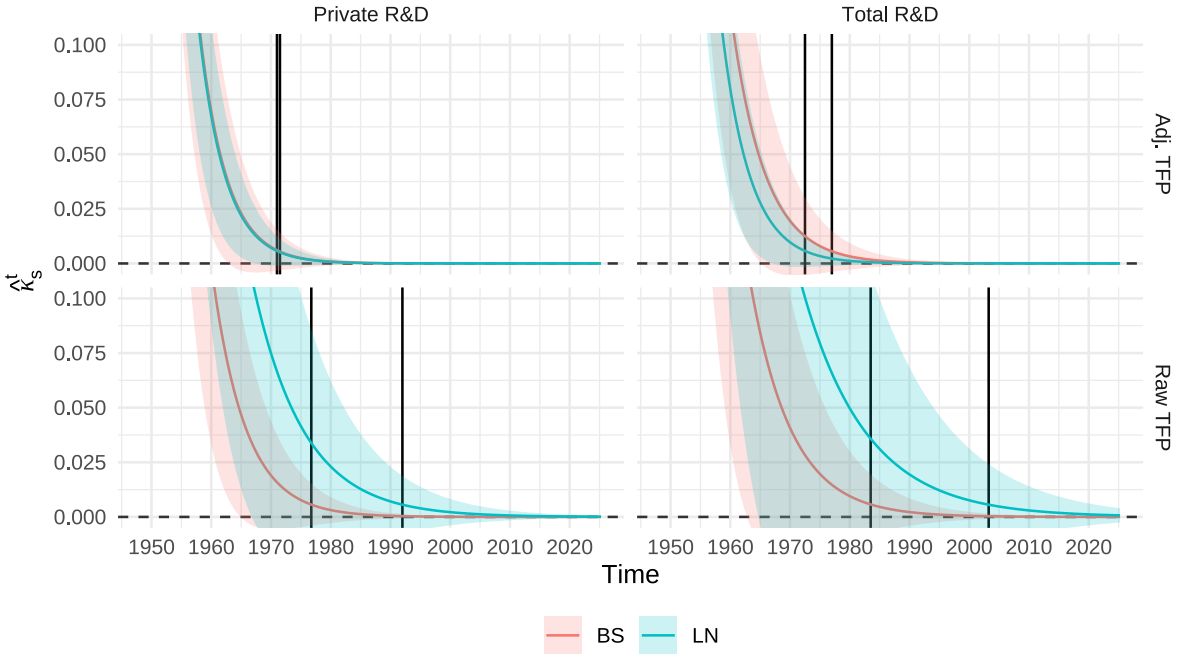


Figure B.4: Implied $\hat{\kappa}_s^t$ for the specifications in Table 2, governing the decay of the unobserved initial condition's influence on the recovered series. Shaded bands are ± 1 standard error; vertical lines mark the trim cutoff τ, for $\gamma = 0.9$.

Appendix B.3. Interpretation of Local Projection Coefficients

From definition (3) and regression (27),

$$b_{c,H,s} \cdot \varepsilon_t^s = \varepsilon_t^x + \Delta\mathbb{E}_t\left(\sum_{j=1}^{H}(1-\kappa_x^j)\,\Delta\ln C_{t+j}\right) - \Delta\mathbb{E}_t\left(\sum_{j=H+1}^{\infty}\kappa_x^j\,\Delta\ln C_{t+j}\right). \tag{B.11}$$

For an arbitrary $\bar{H} > H$, split the residual tail,

$$\Delta\mathbb{E}_t\left(\sum_{j=H+1}^{\infty}\kappa_x^j\,\Delta\ln C_{t+j}\right) = \Delta\mathbb{E}_t\left(\sum_{j=H+1}^{\bar{H}}\kappa_x^j\,\Delta\ln C_{t+j}\right) + \Delta\mathbb{E}_t\left(\sum_{j=\bar{H}+1}^{\infty}\kappa_x^j\,\Delta\ln C_{t+j}\right), \tag{B.12}$$

so that

$$\begin{aligned} b_{c,H,s} \cdot \varepsilon_t^s = \varepsilon_t^x &+ \Delta\mathbb{E}_t\left(\sum_{j=1}^{H}(1-\kappa_x^j)\,\Delta\ln C_{t+j}\right) \\ &- \Delta\mathbb{E}_t\left(\sum_{j=H+1}^{\bar{H}}\kappa_x^j\,\Delta\ln C_{t+j}\right) \\ &- \Delta\mathbb{E}_t\left(\sum_{j=\bar{H}+1}^{\infty}\kappa_x^j\,\Delta\ln C_{t+j}\right). \end{aligned} \tag{B.13}$$

Under suitable conditions, each of the three correction terms is negligible:

$$\kappa_x^H \approx 1 \implies \Delta\mathbb{E}_t\sum_{j=1}^{H}(1-\kappa_x^j)\,\Delta\ln C_{t+j} \approx 0, \tag{B.14}$$

$$b_{c,\hat{H},s} \approx b_{c,H,s} \quad \forall\, H < \hat{H} \le \bar{H} \implies \Delta\mathbb{E}_t\sum_{j=H+1}^{\bar{H}}\kappa_x^j\,\Delta\ln C_{t+j} \approx 0, \tag{B.15}$$

$$\kappa_x^{\bar{H}} \approx 0 \implies \Delta\mathbb{E}_t\sum_{j=\bar{H}+1}^{\infty}\kappa_x^j\,\Delta\ln C_{t+j} \approx 0\,, \tag{B.16}$$

whence

$$b_{c,H,s} \cdot \varepsilon_t^s \approx \varepsilon_t^x\,. \tag{B.17}$$

Appendix C. Empirical Financial Details

Appendix C.1. Financial Data

Appendix C.1.1. Return-Based Analysis (Section 6.1)

The analysis of Section 6.1 draws on three sets of test portfolios. The 153 anomaly portfolios are from Jensen et al. (2021) and the 17 industry-sorted portfolios from Kenneth French's data library. The 13 bond portfolios, spanning maturities of 6 months and 1, 2, 3, 4, 5, 6, 7, 10, 15, 20, 25, and 30 years, are constructed from the zero-coupon yields of Gürkaynak et al. (2007) by fitting Nelson–Siegel–Svensson curves and subtracting the three-month Treasury-bill return.

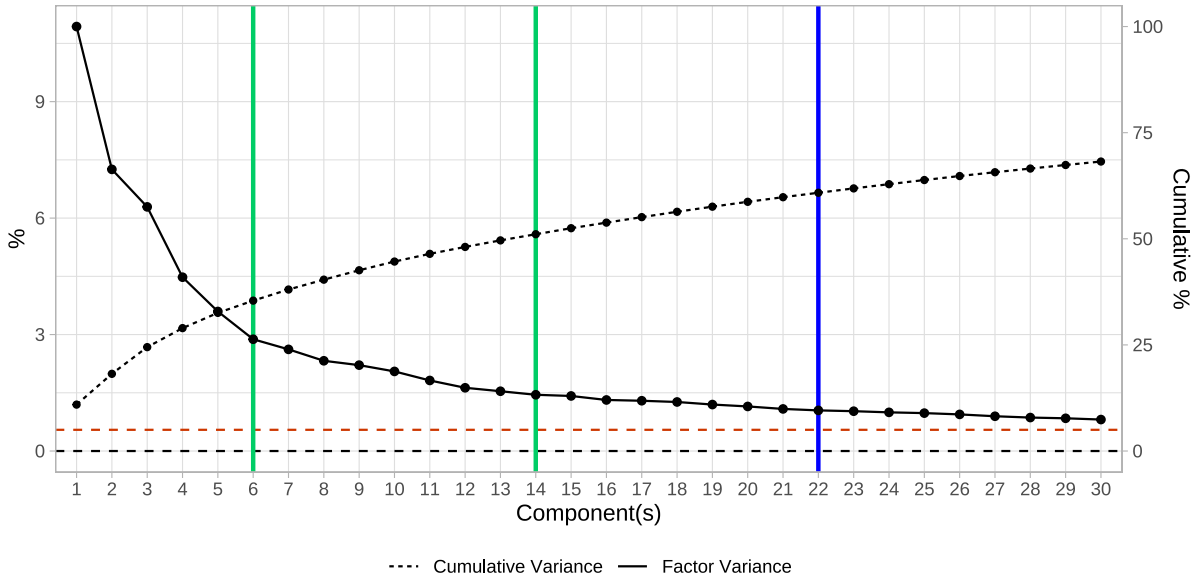


Figure C.5: Principal component scree plot for the test assets of Section 6.1. The solid line (left axis) is the share of return variance explained by each component; the dotted line (right axis) is the cumulative share. The green vertical lines mark the number of factors selected by the two criteria of Alessi et al. (2010), implemented as the median over 300 repetitions; the blue vertical line marks the minimum factor number of Bai and Ng (2002). The horizontal red line is the reciprocal of the number of test assets. The factor count used in the analysis is selected at this stage.

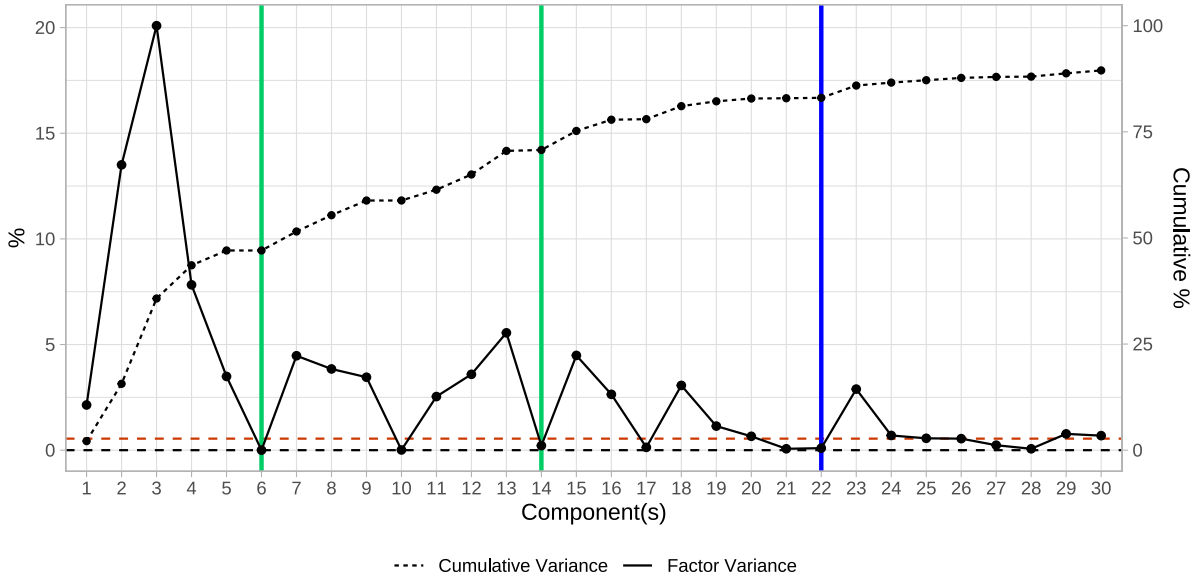


Figure C.6: Variance of cross-sectional average returns explained by the principal components used as risk factors in Section 6.1. The solid line (left axis) is the share explained by each component; the dotted line (right axis) is the cumulative share. The vertical lines reproduce the factor numbers selected at the time-series stage (Figure C.5), shown here only for comparison: selection is not based on cross-sectional fit. The horizontal red line is the reciprocal of the number of test assets.

Appendix C.1.2. Cash-Flow-Based Analysis (Section 6.2)

The payout series is constructed following Bansal et al. (2005) and Hansen et al. (2005). Monthly stock data come from CRSP, and annual accounting data from the Compustat Fundamentals dataset. Monthly returns are compounded to obtain quarterly figures and then deflated using the consumption deflator.

Cash-flow growth rates. First, a measure $h_{i,t}$ of capital gain is computed for each stock by adjusting CRSP ex-dividend returns `RETX` for share repurchases as

$$h_{i,t} = \left(\frac{P_{i,t+1}}{P_{i,t}}\right) \cdot \min\left(\frac{n_{i,t+1}}{n_{i,t}}, 1\right). \tag{C.1}$$

For each portfolio, these stock-level measures are aggregated using market-capitalization weights to obtain a portfolio capital gain series $h_{p,t}$. From each portfolio series, the value of one dollar invested at the beginning of the sample is computed recursively as $V_{p,t+1} = h_{p,t+1}V_{p,t}$ with $V_{p,0} = 1$. Payouts are then given by $D_{p,t+1} = y_{p,t+1}V_{p,t}$, where $y_{p,t+1}$ is the portfolio dividend yield, obtained from $R_{p,t} = h_{p,t} + y_{p,t}$. Capital gains are less than proportional to price appreciation when equivalent shares outstanding decline, typically due to share repurchases, which are a form of payout not recorded in dividend data. Quarterly dividend series are obtained by summing monthly values and deflating them with the implicit price deflator for nondurable and services consumption, constructed as in of Economic Analysis (2024). The series are log-transformed and, following Bansal et al. (2005), de-seasoned with a 4-quarter rolling mean to remove residual seasonality. Finally, cash-flow growth rates are computed as first differences of the log-transformed, de-seasoned real quarterly payouts.

Portfolio Formation. To mitigate liquidity concerns, the sample is restricted to common stocks with market capitalization above the 1st percentile of the monthly NYSE distribution and share price above \$2, which removes less than 0.4% of total market capitalization at any time. Firms must also have at least twelve consecutive observations to enter the sample. Portfolios are formed at the end of June, value-weighted, and held until the following June.

Sorting variables are market capitalization (Size), book-to-market (BM), momentum (Mom), R&D intensity (RD), turnover (To), profitability (Prof), leverage (Lvg), asset growth (AG), Tobin's Q (TQ), and industry (Ind). Most follow a 2×3 sort: stocks are first split at the NYSE median market capitalization, then divided into terciles within each size group. Size, BM, and Mom instead follow univariate sorts, as in Bansal et al. (2005), and Industry is classified directly. Financials (SIC 6000–6999) and utilities (SIC 4000–4999) are excluded where indicated; accounting variables are from the previous fiscal year and market values from the end of calendar year $t-1$.

Size All firms, sorted univariately on market capitalization. Both returns and cash-flow growth decrease with size.

BM Non-financial firms, sorted univariately on book equity over market capitalization. Both returns and cash-flow growth increase with the ratio.

Mom All firms, sorted univariately on cumulative returns from month $t-12$ to month $t-1$. Both returns and cash-flow growth increase with momentum.

RD Non-financial, non-utility firms, sorted on the ratio of R&D expenditure to market capitalization (Chan et al., 2001; Lin, 2011). Returns and cash-flow growth increase with R&D intensity in both the small and the big portfolios.

To All firms, sorted on the sales-to-assets ratio (Haugen and Baker, 1996). Returns and cash-flow growth increase with turnover in both the small and the big portfolios.

Prof Non-financial, non-utility firms, sorted on gross profits over assets (Novy-Marx, 2013; Fama and French, 2015; Hou et al., 2015). Returns and cash-flow growth increase with profitability in both the small and the big portfolios, more strongly among the small.

Lvg Non-financial firms, sorted on the debt-to-assets ratio. Debt-to-assets is used rather than debt-to-market-capitalization, both for consistency with the corporate-finance literature (e.g. Rajan and Zingales, 1995) and with the other financing-related sorts in this study. Returns and cash-flow growth increase with leverage among the small portfolios, while cash-flow growth decreases among the big ones; returns show no clear pattern.

AG Non-financial, non-utility firms, sorted on asset growth, the first difference of assets over its lagged value (Cooper et al., 2008; Hou et al., 2015). Both returns and cash-flow growth decrease with asset growth in both the small and the big portfolios.

TQ All firms, sorted on Tobin's Q, defined as (assets − book equity + market capitalization) / assets as in Chung and Pruitt (1994), following Hou et al. (2015). Cash-flow growth and returns clearly decrease with Tobin's Q in the small portfolios, with no evident pattern in the big ones.

Ind All firms are classified into the 17 industries of Kenneth French's data library, by four-digit SIC code. Returns and cash-flow growth vary across industries with no monotone ordering, by construction.

Table C.4: Descriptive statistics of the legacy pool test assets used in Section 6.2. Quarterly returns and cash-flow growth rates are reported from 1967 Q1 to 2022 Q4; summary statistics include mean and standard deviation.

Portfolio	CF Growth Mean	CF Growth SD	Returns Mean	Returns SD
Size(1)	134.68	604.09	2.47	13.20
Size(2)	68.34	373.78	2.31	11.83
Size(3)	36.33	193.21	2.18	10.77
Size(4)	29.38	161.65	2.14	10.06
Size(5)	6.38	36.26	1.59	8.34
BM(1)	3.09	16.54	1.72	9.76
BM(2)	2.31	21.74	1.78	8.86
BM(3)	1.49	17.17	1.67	8.22
BM(4)	3.47	36.58	1.96	8.65
BM(5)	8.70	69.61	2.41	9.37
Mom(1)	1.11	20.96	1.47	12.61
Mom(2)	7.44	74.50	1.75	9.31
Mom(3)	8.34	58.26	1.78	8.47
Mom(4)	17.24	107.76	1.85	8.77
Mom(5)	34.09	280.68	1.98	11.66

Table C.5: Descriptive statistics of the additional test assets in the wide pool used in Section 6.2. Quarterly returns and cash-flow growth rates are reported from 1967 Q1 to 2022 Q4; summary statistics include mean and standard deviation.

Portfolio	CF Growth Mean	CF Growth SD	Returns Mean	Returns SD
Ind(Cars)	3.71	106.84	2.11	13.17
Ind(Chems)	22.46	433.41	1.87	10.62
Ind(Clths)	6.30	58.46	2.32	13.02
Ind(Cnstr)	26.06	209.55	2.28	11.84
Ind(Cnsum)	28.52	248.93	2.23	8.49
Ind(Durbl)	2.83	62.31	1.17	11.33
Ind(FabPr)	9.56	144.51	1.95	10.75
Ind(Finan)	6.38	49.55	2.03	10.68
Ind(Food)	13.22	113.91	2.18	8.32
Ind(Machn)	49.53	450.87	2.14	12.97
Ind(Mines)	1.46	32.69	1.46	13.13
Ind(Oil)	22.92	186.66	2.09	11.28
Ind(Other)	9.51	50.02	1.78	9.35
Ind(Rtail)	27.08	275.63	2.24	10.67
Ind(Steel)	2.21	48.84	1.50	14.83
Ind(Trans)	3.91	77.20	1.80	10.51
Ind(Utils)	1.51	13.95	1.50	7.51

Table C.6: Descriptive statistics of the additional test assets in the extended pool used in Section 6.2. Quarterly returns and cash-flow growth rates are reported from 1975 Q1 to 2022 Q4; summary statistics include mean and standard deviation.

Portfolio	CF Growth Mean	CF Growth SD	Returns Mean	Returns SD
RD(1-small)	5.23	44.17	2.58	12.32
RD(2-small)	4.53	67.45	2.84	13.13
RD(3-small)	20.34	314.97	4.04	15.79
RD(1-big)	0.97	9.79	1.72	8.42
RD(2-big)	5.90	35.87	2.39	9.02
RD(3-big)	4.04	34.68	2.60	9.69
To(1-small)	3.69	27.70	2.29	10.46
To(2-small)	13.36	73.27	3.01	12.29
To(3-small)	32.86	157.91	3.41	11.99
To(1-big)	0.72	9.65	1.78	8.75
To(2-big)	3.08	18.27	2.08	8.64
To(3-big)	4.88	23.34	2.40	8.62
Prof(1-small)	1.90	42.75	2.29	13.44
Prof(2-small)	15.08	82.61	3.06	12.50
Prof(3-small)	39.22	189.22	3.57	12.47
Prof(1-big)	0.98	10.70	1.75	9.26
Prof(2-big)	3.10	18.54	2.29	8.78
Prof(3-big)	6.87	36.63	2.31	8.70
Lvg(1-small)	4.16	46.37	2.63	12.97
Lvg(2-small)	11.64	87.41	2.97	11.91
Lvg(3-small)	14.02	66.32	3.02	11.99
Lvg(1-big)	2.46	16.73	2.10	9.63
Lvg(2-big)	2.79	17.32	2.15	8.17
Lvg(3-big)	1.70	11.32	2.09	7.92
AG(1-small)	25.67	144.45	3.43	13.38
AG(2-small)	12.67	99.21	2.97	12.37
AG(3-small)	6.93	40.81	2.73	12.37
AG(1-big)	4.67	31.69	2.41	9.08
AG(2-big)	3.33	18.94	2.22	8.18
AG(3-big)	1.47	14.16	1.87	9.25
TQ(1-small)	29.50	248.34	3.45	13.17
TQ(2-small)	16.36	91.69	3.12	12.02
TQ(3-small)	3.18	29.12	2.56	13.60
TQ(1-big)	3.18	26.42	2.18	8.53
TQ(2-big)	2.42	15.68	2.29	8.31
TQ(3-big)	3.05	17.48	1.99	9.94

Table C.7: Cash-flow betas for the legacy-pool portfolios. Each entry is the loading $b^i_{x,D}$ from the time-series regression (28), of portfolio dividend growth on the eight-quarter moving average of the risk factor. The factors are the R&D shock (ε^s), the effective R&D level ($\tilde{s}$), consumption growth (Cons.), and total factor productivity (Prod.). Portfolios are quintiles sorted on size, book-to-market (BM), and past-year returns (Mom). Sample 1967 Q1–2022 Q4.

Portfolio	ε^s	$\tilde{s}$	Cons.	Prod.
Size(1)	1.85	30.84	3.27	3.75
Size(2)	1.63	1.14	1.64	3.20
Size(3)	0.66	−0.35	1.08	1.98
Size(4)	0.48	0.41	0.98	1.40
Size(5)	−0.12	−1.09	0.21	0.36
BM(1)	−0.02	−0.18	0.04	0.09
BM(2)	−0.07	−0.41	0.07	0.14
BM(3)	−0.02	−0.55	0.08	0.12
BM(4)	−0.08	−0.50	0.13	0.23
BM(5)	0.27	0.99	0.30	0.53
Mom(1)	−0.02	−0.19	0.02	0.14
Mom(2)	−0.22	−4.35	0.41	0.44
Mom(3)	0.10	−1.59	0.31	0.41
Mom(4)	−0.18	−1.09	0.35	0.52
Mom(5)	−0.31	−2.58	0.67	1.14

Table C.8: Cash-flow betas for the industry portfolios added in the wide pool. Each entry is the loading $b^i_{x,D}$ from the time-series regression (28), of portfolio dividend growth on the eight-quarter moving average of the risk factor. The factors are the R&D shock (ε^s), the effective R&D level ($\tilde{s}$), consumption growth (Cons.), and total factor productivity (Prod.). Portfolios are the 17 Fama–French industry groups. Sample 1967 Q1–2022 Q4.

Portfolio	ε^s	$\tilde{s}$	Cons.	Prod.
Ind(Cars)	0.35	−1.15	0.40	0.60
Ind(Chems)	0.48	−2.49	0.93	1.38
Ind(Clths)	0.13	−0.08	0.26	0.25
Ind(Cnstr)	0.33	3.55	0.37	1.34
Ind(Cnsum)	−1.10	−2.15	0.19	0.09
Ind(Durbl)	−0.07	−0.99	0.14	0.30
Ind(FabPr)	−0.01	0.17	0.26	0.79
Ind(Finan)	0.01	−1.25	0.33	0.41
Ind(Food)	−0.15	−1.78	0.09	0.59
Ind(Machn)	−0.53	−9.80	1.95	2.66
Ind(Mines)	−0.15	0.37	0.08	0.11
Ind(Oil)	0.38	2.47	1.60	1.76
Ind(Other)	−0.17	−1.28	0.11	0.38
Ind(Rtail)	0.13	−3.61	0.44	1.52
Ind(Steel)	0.11	0.30	0.16	0.19
Ind(Trans)	−0.17	−0.40	0.24	0.24
Ind(Utils)	−0.00	−0.24	0.03	0.07

Table C.9: Cash-flow betas for the characteristic-sorted portfolios of the extended pool. Each entry is the loading $b^i_{x,D}$ from the time-series regression (28), of portfolio dividend growth on the eight-quarter moving average of the risk factor. The factors are the R&D shock (ε^s), the effective R&D level ($\tilde{s}$), consumption growth (Cons.), and total factor productivity (Prod.). Stocks are double-sorted into 2×3 portfolios by size (NYSE median) and one accounting characteristic: firm R&D intensity (RD), profitability (Prof), turnover (To), leverage (Lvg), asset growth (AG), and Tobin Q (TQ); Lo, Mid, Hi (1, 2, 3) index the characteristic terciles, small and big the size halves. Sample 1975 Q1–2022 Q4.

Portfolio	ε^s	$\tilde{s}$	Cons.	Prod.
RD(1-small)	−0.00	−0.51	0.18	0.39
RD(2-small)	−0.02	−0.83	0.04	0.46
RD(3-small)	1.09	−3.03	−0.68	1.17
RD(1-big)	−0.03	−0.30	0.03	0.08
RD(2-big)	−0.07	−0.30	0.12	0.23
RD(3-big)	−0.17	−1.25	0.09	0.24
Prof(1-small)	−0.18	−0.99	−0.01	0.20
Prof(2-small)	0.42	1.15	0.58	0.97
Prof(3-small)	0.71	7.91	1.34	2.29
Prof(1-big)	−0.02	−0.23	0.05	0.09
Prof(2-big)	−0.12	−0.65	0.08	0.16
Prof(3-big)	−0.05	−0.09	0.13	0.34
To(1-small)	0.06	−1.02	0.13	0.27
To(2-small)	0.28	1.34	0.29	0.81
To(3-small)	0.75	5.03	1.06	1.85
To(1-big)	−0.05	−0.47	0.06	0.08
To(2-big)	−0.07	−0.31	0.09	0.17
To(3-big)	0.02	−0.15	0.11	0.29
Lvg(1-small)	−0.09	−0.72	0.15	0.20
Lvg(2-small)	0.17	0.08	0.47	1.03
Lvg(3-small)	0.24	2.17	0.30	0.75
Lvg(1-big)	−0.07	−0.54	0.09	0.19
Lvg(2-big)	−0.08	−0.40	0.08	0.14
Lvg(3-big)	−0.03	−0.07	0.04	0.10
AG(1-small)	0.67	4.25	0.82	1.66
AG(2-small)	−0.07	−0.13	0.43	1.02
AG(3-small)	0.09	0.72	0.19	0.38
AG(1-big)	−0.14	−0.84	0.14	0.29
AG(2-big)	−0.06	−0.51	0.05	0.21
AG(3-big)	−0.04	0.05	0.07	0.08
TQ(1-small)	0.27	2.59	0.87	2.43
TQ(2-small)	0.20	1.31	0.65	1.10
TQ(3-small)	−0.06	−0.39	0.14	0.24
TQ(1-big)	−0.06	−0.39	0.15	0.25
TQ(2-big)	−0.05	−0.52	0.09	0.15
TQ(3-big)	−0.07	−0.00	0.03	0.14

Appendix C.2. Risk Premia Estimation with Omitted Factors

Giglio and Xiu (2021) consider a standard factor structure for returns, of the form

$$\boldsymbol{R}_t - R^f_{t-1} = B\boldsymbol{\lambda} + B\boldsymbol{\epsilon}_t + \boldsymbol{\varphi}_t\,, \tag{C.2}$$

where $\boldsymbol{\epsilon}_t$ are the 'true' risk factors shared by all returns and $\boldsymbol{\varphi}_t$ the idiosyncratic components. The observable factor of interest, x_t, is assumed affine in the true factors, up to measurement error ϖ_t:

$$x_t = \zeta_0 + \boldsymbol{\zeta}_1'\boldsymbol{\epsilon}_t + \varpi_t\,. \tag{C.3}$$

The premium on this factor, λ_x, is the expected excess return on an asset with unit beta on x_t and zero beta on every orthogonal factor:

$$\lambda_x = \boldsymbol{\zeta}_1'\boldsymbol{\lambda}\,. \tag{C.4}$$

Consistent estimates of λ_x, free of the omitted-factor bias, are obtained by applying principal component analysis to the panel of returns, which recovers the true risk factors up to an arbitrary full-rank rotation H, namely $H\boldsymbol{\epsilon}_t$, as the number of periods and test assets grows. Regressing $\boldsymbol{R}_t$ on the estimated $\widehat{H\boldsymbol{\epsilon}_t}$ then yields consistent estimates of $\boldsymbol{\zeta}_1'H^{-1}$. These, in turn, serve as regressors for $\boldsymbol{R}_t$, as in the classical Fama–MacBeth procedure (Fama and Macbeth, 1973), giving consistent estimates of $H\boldsymbol{\lambda}$. Combining the two yields the consistent estimate

$$\hat{\lambda}_x = \widehat{\boldsymbol{\zeta}_1'H^{-1}}\,\widehat{H\boldsymbol{\lambda}}\,, \tag{C.5}$$

in which the rotation H cancels, leaving $\hat{\lambda}_x$ invariant to it.

Appendix C.3. Cash-Flow-Based Asset Pricing

According to the arguments presented in the main text, Bansal et al. (2005) adopt the simpler cross-sectional pricing condition

$$\mathbb{E}_t\left[R^i_{t+1}\right] - R^f_t = \lambda_x\beta^i_x \tag{C.6}$$

as a reasonable approximation of the theoretical long-run risk pricing equation. Then, decomposing unexpected returns into a sum of news about future cash-flow growth and of discount rates as in Campbell (1996),

$$\ln R^i_{t+1} - \mathbb{E}_t\left[\ln R^i_{t+1}\right] \approx \delta^i_{D,t+1} - \delta^i_{R,t+1} \tag{C.7}$$

where

$$\delta^i_{D,t} = \{\mathbb{E}_t - \mathbb{E}_{t-1}\}\left[\sum_{j=0}^{\infty}\bar{\kappa}^j\Delta\ln D^i_{t+j}\right]\,,\quad \delta^i_{R,t} = \{\mathbb{E}_t - \mathbb{E}_{t-1}\}\left[\sum_{j=1}^{\infty}\bar{\kappa}^j\ln R^i_{t+j}\right]\,, \tag{C.8}$$

any return beta can be approximated as the difference between a cash-flow beta, $\beta^i_{x,D}$, and a discount-rate beta, $\beta^i_{x,R}$ (Campbell and Vuolteenaho, 2004):

$$\beta^i_x = \frac{\mathrm{Cov}\left[R^i_t\,,\,\varepsilon_{x,t}\right]}{\mathrm{Var}\left[\varepsilon_{x,t}\right]} \approx \frac{\mathrm{Cov}\left[\delta^i_{D,t}\,,\,\varepsilon_{x,t}\right]}{\mathrm{Var}\left[\varepsilon_{x,t}\right]} - \frac{\mathrm{Cov}\left[\delta^i_{R,t}\,,\,\varepsilon_{x,t}\right]}{\mathrm{Var}\left[\varepsilon_{x,t}\right]} = \beta^i_{x,D} - \beta^i_{x,R}\,. \tag{C.9}$$

Focusing on the dividend beta alone isolates the component of risk stemming from assets' fundamentals, yielding

$$\mathbb{E}_t\left[R^i_{t+1}\right] - R^f_t = \lambda_x\beta^i_{x,D}\,. \tag{C.10}$$

Appendix D. Additional Results

Appendix D.1. Related Measures

By construction and purpose of use, the closest measure in the literature is from Kung and Schmid (2015). They focused on a specification of effective R&D defined as the plain ratio S_t/I_t. The empirical counterpart was constructed as the ratio of U.S. annual private R&D expenditures reported by the National Science Foundation (measuring S_t) to the R&D stock series formed by the U.S. Bureau of Labor Statistics (representing intangible capital I_t). They showed that this measure fulfilled several theoretical predictions: it was highly persistent, co-moved at low frequencies with the price-dividend ratio, and univariately forecasted the growth of consumption, GDP, and TFP up to 5 years.

Their measure, however, presents a few shortcomings, illustrated in the first column of Table D.10.[2] Most notably, it is extremely persistent, with a first-order annual autocorrelation of 0.995 (standard error 0.063). This raises two concerns: the upper confidence bound indicates a real risk of non-stationarity, while the lower implies persistence too high for the productivity component it should capture. Formal tests conflict: ADF rejects non-stationarity at 10%, KPSS rejects stationarity at 1%, with visual inspection favoring the latter. Non-stationarity would not undermine the measure or the underlying theory, but it would pose serious problems for empirical work, given the risk of spurious regressions. Even setting stationarity aside, an implied half-life exceeding 40 years strains its economic interpretation. This far exceeds the persistence of the productivity LRR component in Ortu et al. (2013) and Croce (2014), which never exceeds 20 years. Though consistent with the consumption-based calibration of Bansal and Yaron (2004), it appears too long-lived to reflect the productivity channel of long-run risk.

The puzzling dynamics of the effective R&D used by Kung and Schmid (2015) may stem from the data employed, as the measure of the stock of ideas they use is constructed through simple accumulation and depreciation of R&D expenditures, deviating from the law of motion assumed in the model. To address this inconsistency, one could construct an alternative effective R&D measure by substituting TFP for the stock of ideas (as previously argued), maintaining the assumption of labor-augmenting technology, and calibrating it using standard labor share values from the literature, as well as employing the longer datasets used in this work. However, the results exhibit similar, if not more pronounced, issues (see Table D.10). The root cause likely lies in the lack of flexibility in the strength of knowledge spillovers from past innovations in the Kung and Schmid (2015) framework, a limitation that recent work, such as Bloom et al. (2020), has highlighted as crucial for achieving a good empirical fit to the data.

Another closely related measure is proposed by Kogan et al. (2017), who link changes in market valuations to patent announcements to assess the private value of successful innovations. Whereas their measure captures the outcome of the innovation process, effective R&D reflects its input side. The two measures thus offer complementary perspectives on innovation. For the purposes of this paper, however – namely, constructing a process that forecasts future innovation and productivity growth – effective R&D is particularly suitable. This is further supported by the results in Table D.11, which show that structural R&D shocks from effective R&D Granger-cause the structural innovation shocks from innovation measure of Kogan et al. (2017), but not vice versa, for most specifications.

[2]The R&D stock series has been updated by the provider and now covers a slightly different period.

Table D.10: Summary statistics of the (updated) Kung and Schmid (2015) R&D intensity measure. Column 1 reports yearly R&D expenditure (S, NSF) and R&D stock (I, BLS) for 1963-2020 (yearly observations from 1986 onward); columns 2-3 show data from the baseline specifications in the main analysis. θ corresponds to commonly used labor-share values, following the original paper. T denotes the number of observations; σ, the standard deviation; *ADF* and *KPSS*, respective stationarity tests; *AR(1)*, the first-order autoregressive coefficient; and *HL*, the implied half-life based on AR(1).

$\tilde{s}_t$:	$(\ln S_t - \ln I_t)$	$(\ln S_t - \frac{1}{\theta} \ln Z_t)$	
$1-\theta$:	–	0.35	0.3
T	62	314	314
σ	0.321	0.864	0.835
ADF	-2.82^{*}	3.80	3.72
KPSS	1.29^{***}	0.82^{***}	0.79^{***}
AR(1)	0.995^{***}	1.000^{***}	1.000^{***}
	(0.063)	(0.000)	(0.000)
HL low	40.2	∞	∞
HL high	∞	∞	∞

$^{***}p < 0.01$, $^{**}p < 0.05$, $^{*}p < 0.1$

Table D.11: Granger causality F-test p-values from a VAR of effective R&D (s) and the aggregated innovation measure of Kogan et al. (2017) (KPSS), both included as structural shocks orthogonal to productivity growth, estimated from a first-step bivariate VAR with productivity growth (as in Table 3). VAR lags are selected by Hannan–Quinn information criterion (max 10); k denotes second-step VAR lags. Results are shown using HC, and HAC covariance estimators.

	Baseline	S: Tot. R&D	Z: Raw TFP	Q: N.F. Empl.	$\tilde{s}$
k	1	1	2	1	1
N. Obs.	298	298	298	298	216
GC(s) HC p.v.	0.069	0.934	0.068	0.072	0.079
GC(KPSS) HC p.v.	0.838	0.436	0.864	0.745	0.233
GC(s) HAC p.v.	0.011	0.921	0.010	0.008	0.012
GC(KPSS) HAC p.v.	0.824	0.497	0.864	0.719	0.083

$^{***}p < 0.01$, $^{**}p < 0.05$, $^{*}p < 0.1$

Appendix D.2. Three-Shock Structural System

This section assumes, instead of (18),

$$\tilde{s}_{t+1} = \rho_s \tilde{s}_t + \beta_{s,a} a_t + \beta_{s,L} \widetilde{\Delta \ln L}_t + \delta_{s,L} \varepsilon^L_{t+1} + \delta_{s,a} \varepsilon^a_{t+1} + \delta_{s,s} \varepsilon^s_{t+1} \tag{D.1a}$$

$$a_{t+1} = \beta_{a,s} \tilde{s}_t + \rho_a a_t + \beta_{a,L} \widetilde{\Delta \ln L}_t + \delta_{a,L} \varepsilon^L_{t+1} + \delta_{a,a} \varepsilon^a_{t+1} \tag{D.1b}$$

$$\widetilde{\Delta \ln L}_{t+1} = \beta_{L,s} \tilde{s}_t + \beta_{L,a} a_t + \rho_L \widetilde{\Delta \ln L}_t + \delta_{L,L} \varepsilon^L_{t+1} + \delta_{L,a} \varepsilon^a_{t+1} \,. \tag{D.1c}$$

Appendix D.2.1. Short-Run System in Observables

Substituting (A.22) in

$$\Delta a_{t+1} = \beta_{a,s} \tilde{s}_t + (\rho_a - 1) a_t + \beta_{a,L} \widetilde{\Delta \ln L}_t + \delta_{a,L} \varepsilon^L_{t+1} + \delta_{a,a} \varepsilon^a_{t+1} \tag{D.2}$$

from (D.1b), yields

$$\Delta a_{t+1} = \beta_{a,s} \hat{s}_t + \left(\rho_a - 1 + \beta_{a,s} \left(\alpha_Z + \alpha_L \cdot \frac{\pi}{\omega} \right) \right) a_t + \beta_{a,L} \widetilde{\Delta \ln L}_t + \delta_{a,L} \varepsilon^L_{t+1} + \delta_{a,a} \varepsilon^a_{t+1} \,. \tag{D.3}$$

Then, first, substituting (A.22) into (D.1c),

$$\begin{aligned} \widetilde{\Delta \ln L}_{t+1} = {} & \beta_{L,s} \hat{s}_t + \beta_{L,s} \left[\left(\alpha_Z + \alpha_L \cdot \frac{\pi}{\omega} \right) + \beta_{L,a} \right] a_t \\ & + \rho_L \widetilde{\Delta \ln L}_t + \delta_{L,L} \varepsilon^L_{t+1} + \delta_{L,a} \varepsilon^a_{t+1} \,. \end{aligned} \tag{D.4}$$

Second, substituting Δa_{t+1} from (D.2) and $\widetilde{\Delta \ln L}_{t+1}$ from (D.1c) into (A.26),

$$\begin{aligned} \widetilde{\Delta \ln Z}_{t+1} \approx {} & \gamma_0 + \left(\gamma_1 + \xi\omega\beta_{L,s} + (1+\xi\pi)\beta_{a,s} \right) \tilde{s}_t \\ & + \left[\xi\omega\beta_{L,a} + (1+\xi\pi)(\rho_a - 1) \right] a_t + \left[\xi\omega\rho_L + (1+\xi\pi)\beta_{a,L} \right] \widetilde{\Delta \ln L}_t \\ & + \left[\xi\omega\delta_{L,L} + (1+\xi\pi)\delta_{a,L} \right] \varepsilon^L_{t+1} + \left[\xi\omega\delta_{L,a} + (1+\xi\pi)\delta_{a,a} \right] \varepsilon^a_{t+1} \,, \end{aligned} \tag{D.5}$$

which, plugging (A.22) in, amounts to

$$\begin{aligned} \widetilde{\Delta \ln Z}_{t+1} \approx {} & \gamma_0 + \left(\gamma_1 + \xi\omega\beta_{L,s} + (1+\xi\pi)\beta_{a,s} \right) \hat{s}_t \\ & + \left[\left(\gamma_1 + \xi\omega\beta_{L,s} + (1+\xi\pi)\beta_{a,s} \right) \left(\alpha_Z + \alpha_L \cdot \frac{\pi}{\omega} \right) + \xi\omega\beta_{L,a} + (1+\xi\pi)(\rho_a - 1) \right] a_t \\ & + \left[\xi\omega\rho_L + (1+\xi\pi)\beta_{a,L} \right] \widetilde{\Delta \ln L}_t \\ & + \left[\xi\omega\delta_{L,L} + (1+\xi\pi)\delta_{a,L} \right] \varepsilon^L_{t+1} + \left[\xi\omega\delta_{L,a} + (1+\xi\pi)\delta_{a,a} \right] \varepsilon^a_{t+1} \,. \end{aligned} \tag{D.6}$$

Third, further substituting (A.22) into (D.1a),

$$\begin{aligned} \hat{s}_{t+1} + \left(\alpha_Z + \alpha_L \cdot \frac{\pi}{\omega} \right) \Delta a_{t+1} = {} & \rho_s \hat{s}_t + \left[(\rho_s - 1) \left(\alpha_Z + \alpha_L \cdot \frac{\pi}{\omega} \right) + \beta_{s,a} \right] a_t + \beta_{s,L} \widetilde{\Delta \ln L}_t \\ & + \delta_{s,L} \varepsilon^L_{t+1} + \delta_{s,a} \varepsilon^a_{t+1} + \delta_{s,s} \varepsilon^s_{t+1} \,, \end{aligned} \tag{D.7}$$

which, with (D.3),

$$\begin{aligned}\hat{s}_{t+1} = &\left(\rho_s - \left(\alpha_Z + \alpha_L \cdot \frac{\pi}{\omega}\right)\beta_{a,s}\right)\hat{s}_t \\ &+ \left[(\rho_s - 1)\left(\alpha_Z + \alpha_L \cdot \frac{\pi}{\omega}\right) + \beta_{s,a} - \left(\alpha_Z + \alpha_L \cdot \frac{\pi}{\omega}\right)\left(\rho_a - 1 + \beta_{a,s}\left(\alpha_Z + \alpha_L \cdot \frac{\pi}{\omega}\right)\right)\right] a_t \\ &+ \left(\beta_{s,L} - \left(\alpha_Z + \alpha_L \cdot \frac{\pi}{\omega}\right)\beta_{a,L}\right)\widetilde{\Delta \ln L_t} \\ &+ \left(\delta_{s,L} - \left(\alpha_Z + \alpha_L \cdot \frac{\pi}{\omega}\right)\delta_{a,L}\right)\varepsilon^L_{t+1} + \left(\delta_{s,a} - \left(\alpha_Z + \alpha_L \cdot \frac{\pi}{\omega}\right)\delta_{a,a}\right)\varepsilon^a_{t+1} + (\delta_{s,s})\,\varepsilon^s_{t+1}\,.\end{aligned} \tag{D.8}$$

Fourth, plugging (A.22) in (D.1b), a_t can be rewritten as

$$a_{t+1} = \beta_{a,s}\hat{s}_t + \left[\rho_a + \beta_{a,s}\left(\alpha_Z + \alpha_L \cdot \frac{\pi}{\omega}\right)\right] a_t + \beta_{a,L}\widetilde{\Delta \ln L_t} + \delta_{a,L}\varepsilon^L_{t+1} + \delta_{a,a}\varepsilon^a_{t+1}\,. \tag{D.9}$$

Finally, the system (D.1) can then be expressed as

$$\begin{bmatrix}\boldsymbol{x}_{t+1} \\ a_{t+1}\end{bmatrix} = \begin{pmatrix}B_{x,x} & \boldsymbol{b}_{x,a} \\ \boldsymbol{b}'_{a,x} & b_{a,a}\end{pmatrix}\begin{bmatrix}\boldsymbol{x}_t \\ a_t\end{bmatrix} + \begin{pmatrix}D_x \\ \boldsymbol{d}'_a\end{pmatrix}\boldsymbol{\varepsilon}_{t+1}\,, \tag{D.10}$$

where $\boldsymbol{x}_t$ is $\left[\hat{s}_t,\, \widetilde{\Delta \ln Z_t}, \widetilde{\Delta \ln L_t}\right]'$ and $\boldsymbol{\varepsilon}_{t+1}$ is $[\varepsilon^s_{t+1}\,, \varepsilon^a_{t+1},\, \varepsilon^L_{t+1}]'$. $B_{x,x}$, $\boldsymbol{b}_{x,a}$, D_x, $\boldsymbol{b}_{a,x}$, $b_{a,a}$ and $\boldsymbol{d}_a$ are all defined across (D.8), (D.6), (D.4), and (D.9). So,

$$\boldsymbol{x}_{t+1} = B_{x,x}\boldsymbol{x}_t + \boldsymbol{b}_{x,a}a_t + D_x\boldsymbol{\varepsilon}_{t+1}\,, \tag{D.11}$$

and

$$a_{t+1} = \boldsymbol{b}'_{a,x}\boldsymbol{x}_t + b_{a,a}a_t + \boldsymbol{d}'_a\boldsymbol{\varepsilon}_{t+1}\,. \tag{D.12}$$

Then, plugging the lag of (D.12) in (D.11),

$$\begin{aligned}\boldsymbol{x}_{t+1} = &B_{x,x}\boldsymbol{x}_t + \boldsymbol{b}_{x,a}\boldsymbol{b}'_{a,x}\boldsymbol{x}_{t-1} + b_{a,a}(\boldsymbol{b}_{x,a}a_{t-1}) \\ &+ D_x\boldsymbol{\varepsilon}_{t+1} + \boldsymbol{b}_{x,a}\boldsymbol{d}'_a\boldsymbol{\varepsilon}_t\,,\end{aligned} \tag{D.13}$$

and using the lag of (D.11)

$$\boldsymbol{b}_{x,a}a_{t-1} = \boldsymbol{x}_t - B_{x,x}\boldsymbol{x}_{t-1} - D_x\boldsymbol{\varepsilon}_t\,, \tag{D.14}$$

yields

$$\begin{aligned}\boldsymbol{x}_{t+1} = &(B_{x,x} + I_x b_{a,a})\boldsymbol{x}_t + (\boldsymbol{b}_{x,a}\boldsymbol{b}'_{a,x} - b_{a,a}B_{x,x})\boldsymbol{x}_{t-1} \\ &+ D_x\boldsymbol{\varepsilon}_{t+1} + (\boldsymbol{b}_{x,a}\boldsymbol{d}'_a - b_{a,a}D_x)\boldsymbol{\varepsilon}_t\,,\end{aligned} \tag{D.15}$$

which expands to

$$\begin{aligned}\begin{bmatrix}\widetilde{\hat{s}_{t+1}} \\ \widetilde{\Delta \ln Z_{t+1}} \\ \widetilde{\Delta \ln L_{t+1}}\end{bmatrix} = &B_1\begin{bmatrix}\widetilde{\hat{s}_t} \\ \widetilde{\Delta \ln Z_t} \\ \widetilde{\Delta \ln L_t}\end{bmatrix} + B_2\begin{bmatrix}\widetilde{\hat{s}_{t-1}} \\ \widetilde{\Delta \ln Z_{t-1}} \\ \widetilde{\Delta \ln L_{t-1}}\end{bmatrix} \\ &+ \begin{pmatrix}\delta^1_{s,s} & \delta^1_{s,a} & \delta^1_{s,L} \\ 0 & \delta^1_{Z,a} & \delta^1_{Z,L} \\ 0 & \delta^1_{L,a} & \delta^1_{L,L}\end{pmatrix}\begin{bmatrix}\varepsilon^s_{t+1} \\ \varepsilon^a_{t+1} \\ \varepsilon^L_{t+1}\end{bmatrix} + \begin{bmatrix}\varepsilon^s_t \\ \varepsilon^a_t \\ \varepsilon^L_t\end{bmatrix}\,.\end{aligned} \tag{D.16}$$

Appendix D.2.2. Empirical Results

All key results for the finite-order VAR approximating (D.16) are reported in Table D.12, Figures D.7 and D.8, and Table D.13. Effective R&D remains strongly predictive of TFP growth, and the Granger-causality test remains significant; structural R&D shocks are highly correlated with those from the corresponding two-variable specifications and yield nearly identical impulse responses. The consumption local projection is less precisely estimated, but still stabilizes around a positive value after roughly six years, as in the main specification. The pricing estimates overlap with those in the main text.

Table D.12: Estimation diagnostics for the three-variable finite-order VAR approximating (D.16), which augments the system of (25) with labor-force growth. Columns, statistics, and tests are as in Table 3. $\hat{v}^s$ *corr. (2v, 3v)* is the correlation between the structural R&D shock estimates from the three- and two-variable systems, for each specification.

	Baseline	S: Tot. R&D	Z: Raw TFP	L: N.F. Empl.	s: Net
T	306	305	304	306	216
P	2	3	4	2	2
$R^2_{\Delta Z}$ (%)	6.5	6.4	11.6	5.8	3.1
max |roots|	0.93	0.88	0.95	0.94	0.94
ARCH-LM($\Delta Z, 4$)	2.3	1.5	22.0***	2.7	3.7
ARCH-LM($s, 4$)	49.4***	40.9***	43.3***	52.1***	20.0***
AC-LM(1)	9.7	12.7	5.8	9.4	9.8
AC-LM(4)	43.3	44.5	35.7	39.5	45.6
AC-LM(16)	157.4	151.2	133.1	157.5	139.4
AC-LM(40)	294.5	288.0	281.6	294.6	204.9
GC-F(s)	17.8***	11.8***	3.1***	18.6***	1.8
$\hat{v}^s$ corr. (2v, 3v)	0.86	0.92	0.88	0.83	0.95

$^{***}p < 0.01$, $^{**}p < 0.05$, $^{*}p < 0.1$

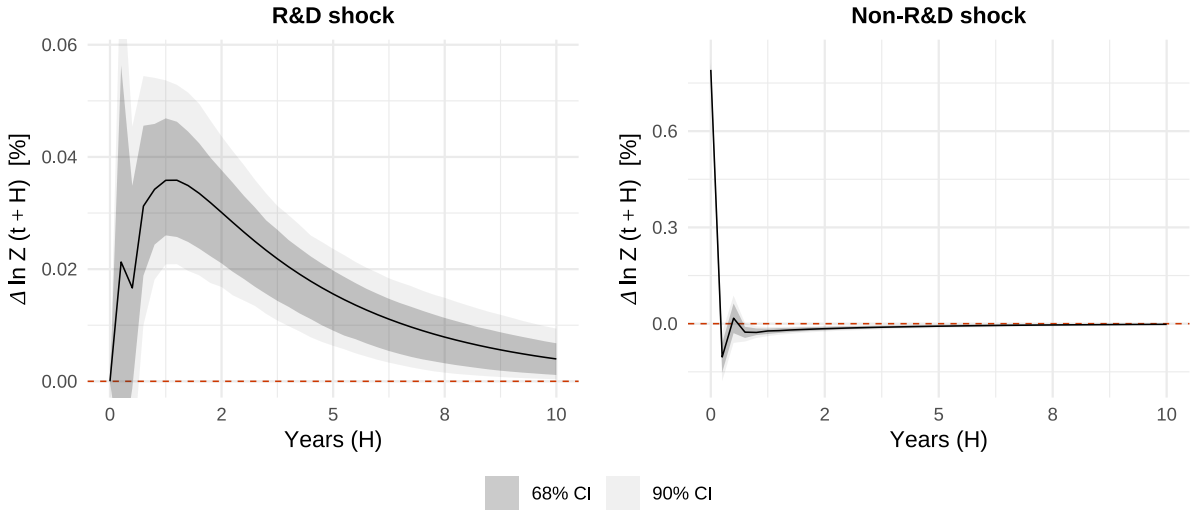


Figure D.7: Impulse response functions from the baseline three-variable finite-order VAR approximating (D.16), which augments the system of (25) with labor-force growth. The left panel reports the response of $\Delta \ln Z$ to a one-standard-deviation R&D shock (ε^s_t) and the right panel the response to a one-standard-deviation non-R&D shock (ε^a_t); bootstrap, specification, and horizon are as in Figure 3.

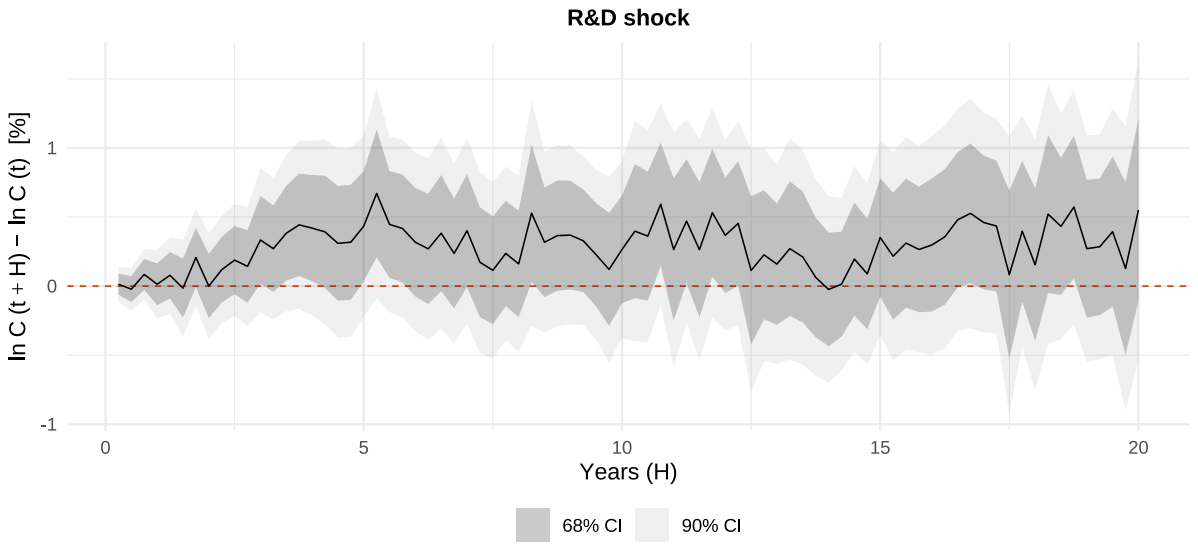


Figure D.8: Cumulative impulse response of consumption growth ($\Delta \ln C$) to the R&D shock ($\hat{\varepsilon}^s$) identified from the three-variable finite-order VAR approximating (D.16), from the local projection of (27) ($P = 5$). Bands and horizon are as in Figure 4.

Table D.13: Cash-flow risk premia λ_x with the R&D shock identified from the three-variable finite-order VAR approximating (D.16). Construction, test assets, and sample are as in Table 4.

	Baseline	S: Tot. R&D	Z: Raw TFP	L: N.F. Empl.	s: Net
			Horizon: 1 quarter		
6 factors	4.73	6.54	6.38	5.17	7.47
	[0.83]	[1.23]	[1.12]	[0.89]	[1.05]
14 factors	13.22	9.55	6.09	12.73	9.31
	[0.98]	[0.68]	[0.43]	[0.93]	[0.54]
T	213	213	213	213	213
			Horizon: 4 years		
6 factors	2.01	2.31	1.90	2.17	2.10
	[1.42]	[1.58]	[1.05]	[1.50]	[0.80]
14 factors	10.38***	7.95**	12.52***	9.92***	16.72***
	[3.10]	[2.56]	[3.23]	[2.90]	[2.90]
T	213	213	213	213	199

$^{***}p < 0.01$, $^{**}p < 0.05$, $^{*}p < 0.1$

Appendix D.3. Other Tables

This subsection presents supplementary correlation tables for three objects implied by estimates in the main text: the error-correction terms from the cointegration estimates of Table 1 (Table D.14), the effective R&D levels from the regressions of Table 2 (Table D.15), and the structural R&D shocks from the VAR of Table 3 (Table D.16).

Table D.14: Correlation among error correction terms from the specifications in Table 1.

	Baseline	S: Tot. R&D	Z: Raw TFP	L: N.F. Empl.
S: Tot. R&D	0.88	.	.	.
Z: Raw TFP	0.86	0.72	.	.
Q: N.F. Empl.	1.00	0.86	0.86	.
Est. Meth.: IM	0.51	0.50	0.38	0.50

Table D.15: Correlation among estimates of $\tilde{s}_t$ from the specifications in Table 2.

Specification	Baseline	S: Tot. R&D	Z: Raw TFP	L: N.F. Empl.
S: Tot. R&D	0.75	.	.	.
Z: Raw TFP	0.96	0.64	.	.
L: N.F. Empl.	1.00	0.76	0.96	.
Baseline-BS	1.00	0.75	0.96	1.0

Table D.16: Correlation among estimates of structural shocks from the VAR specifications in Table 3.

	Baseline	S: Tot. R&D	Z: Raw TFP	L: N.F. Empl.
S: Tot. R&D	0.69	.	.	.
Z: Raw TFP	0.90	0.60	.	.
L: N.F. Empl.	0.99	0.70	0.89	.
s : Net	0.61	0.65	0.63	0.61

$^{***}p < 0.01$, $^{**}p < 0.05$, $^{*}p < 0.1$

Appendix D.4. Other Figures

This subsection collects the figures underlying the main-text estimates. Figure D.9 plots the error-correction terms from all estimated cointegration relationships, and Figure D.10 the effective R&D levels $\hat{\tilde{s}}_t$ from all tested specifications, with the structural R&D shocks $\hat{\varepsilon}^s_t$ from the baseline VAR shown in Figure D.11. Figure D.12 reports the responses of effective R&D, both gross and net, to a non-R&D TFP shock, and Figure D.13 the AIC of the local projections across lag lengths, underlying the lag choice for the cumulative impulse responses.

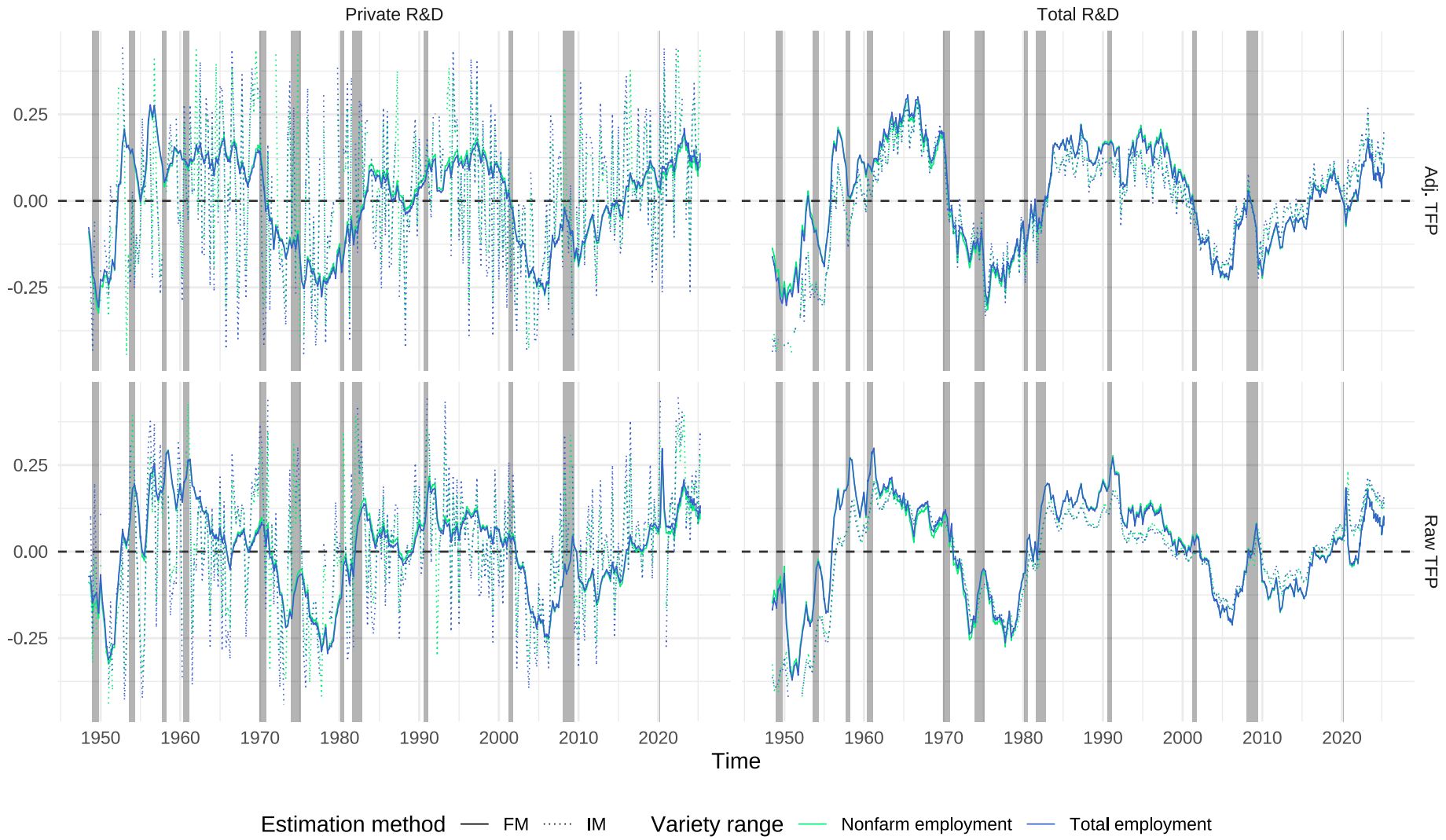


Figure D.9: Error correction terms from all estimated cointegration relationships; selected relationships are reported in Table 1. Shaded areas indicate NBER recessions.



Figure D.10: $\hat{\hat{s}}_t$ from all tested specifications. The construction of the series and the confidence intervals are described in Appendix B.2. Shaded areas indicate NBER recessions.

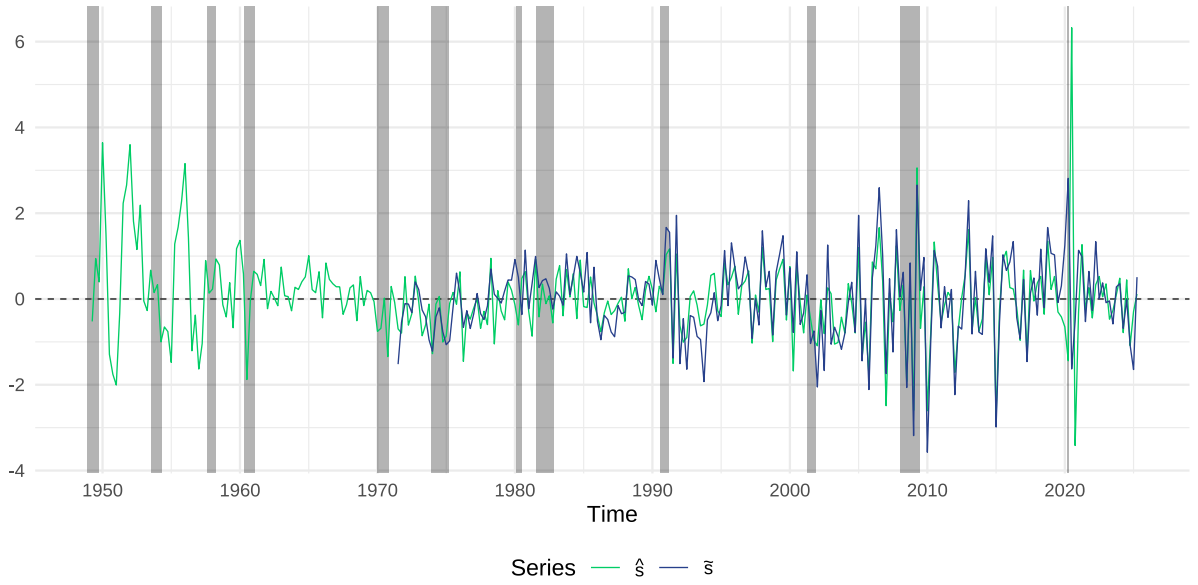


Figure D.11: $\hat{v}_t^s$ from baseline VAR estimation in Table 3. Shaded areas indicate NBER recessions.

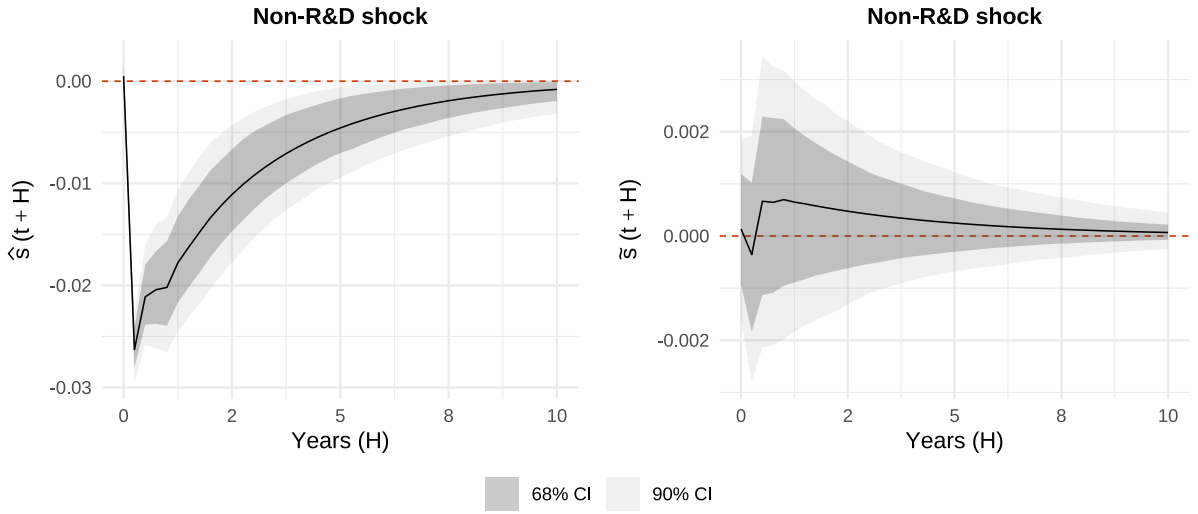


Figure D.12: Impulse response functions to a one-standard-deviation non-R&D TFP shock (ε_t^a) from the VAR in (25) (cf. Table 3). The left panel reports the response of $\hat{s}_t$ under the baseline gross specification; the right panel reports the response of $\tilde{s}_t$ under the net specification. Dark and light shaded areas show 68% and 90% percentile intervals from a residual bootstrap with 1,099 replications. The horizon H is expressed in years.

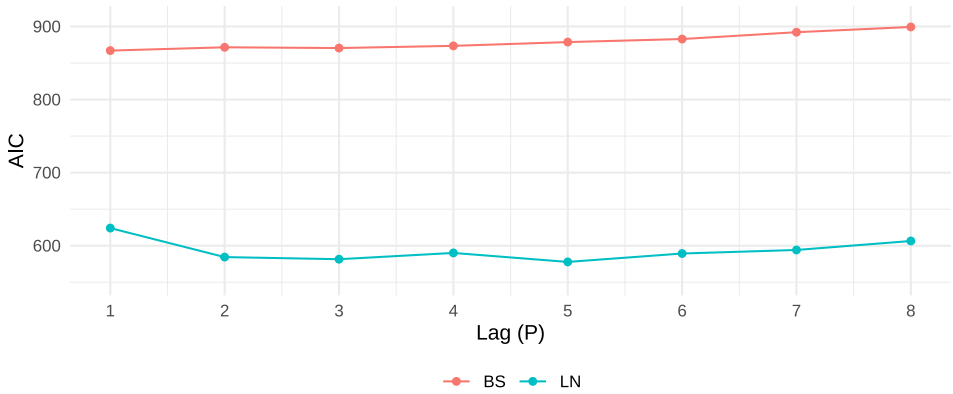


Figure D.13: AIC of the local projection regressions across lag lengths P, for productivity and consumption, underlying the lag choice for the cumulative impulse responses in Figure 4.

References

Ai, H., Croce, M.M., Diercks, A.M., Li, K., 2018. News shocks and the production-based term structure of equity returns. The Review of Financial Studies 31, 2423–2467. doi:10.1093/rfs/hhy015.

Alessi, L., Barigozzi, M., Capasso, M., 2010. Improved penalization for determining the number of factors in approximate factor models. Statistics & Probability Letters 80, 1806–1813. doi:10.1016/j.spl.2010.08.005.

Bai, J., Ng, S., 2002. Determining the Number of Factors in Approximate Factor Models. Econometrica 70, 191–221. doi:10.1111/1468-0262.00273.

Bansal, R., Dittmar, R.F., Lundblad, C.T., 2005. Consumption, dividends, and the cross section of equity returns. The Journal of Finance 60, 1639–1672. doi:10.1111/j.1540-6261.2005.00776.x.

Bansal, R., Shaliastovich, I., 2013. A long-run risks explanation of predictability puzzles in bond and currency markets. Review of Financial Studies 26, 1–33. doi:10.1093/rfs/hhs108.

Bansal, R., Yaron, A., 2004. Risks for the Long Run: A Potential Resolution of Asset Pricing Puzzles. The Journal of Finance 59, 1481–1509. doi:10.1111/j.1540-6261.2004.00670.x.

Bloom, N., Jones, C.I., Van Reenen, J., Webb, M., 2020. Are ideas getting harder to find? American Economic Review 110, 1104–1144. doi:10.1257/aer.20180338.

Campbell, J.Y., 1996. Understanding risk and return. Journal of Political Economy 104, 298–345. doi:10.1086/262026.

Campbell, J.Y., Vuolteenaho, T., 2004. Bad Beta, Good Beta. American Economic Review 94, 1249–1275. doi:10.1257/0002828043052240.

Chan, L.K.C., Lakonishok, J., Sougiannis, T., 2001. The stock market valuation of research and development expenditures. Journal of Finance 56, 2431–2456. doi:10.1111/0022-1082.00411.

Chung, K.H., Pruitt, S.W., 1994. A simple approximation of tobin's q. Financial Management 23, 70. doi:10.2307/3665623.

Cooper, M.J., Gulen, H., Schill, M.J., 2008. Asset Growth and the Cross-Section of Stock Returns. The Journal of Finance 63, 1609–1651. doi:10.1111/j.1540-6261.2008.01370.x.

Croce, M.M., 2014. Long-run productivity risk: A new hope for production-based asset pricing? Journal of Monetary Economics 66, 13–31. doi:10.1016/j.jmoneco.2014.04.001.

of Economic Analysis, B., 2024. Chapter 4: Estimating methods, in: NIPA Handbook: Concepts and Methods of the U.S. National Income and Product Accounts. U.S. Department of Commerce, Bureau of Economic Analysis. chapter 4.

Fama, E.F., French, K.R., 2015. A five-factor asset pricing model. Journal of Financial Economics 116, 1–22. doi:10.1016/j.jfineco.2014.10.010.

Fama, E.F., Macbeth, J.D., 1973. Risk, return, and equilibrium: Empirical tests. Journal of Political Economy 81, 607–636.

Fernald, J.G., 2012. A quarterly, utilization-adjusted series on total factor productivity. Federal Reserve Bank of San Francisco, Working Paper Series , 1–28doi:10.24148/wp2012-19.

Giglio, S., Xiu, D., 2021. Asset pricing with omitted factors. Journal of Political Economy 129, 1947–1990. doi:10.1086/714090.

Gürkaynak, R.S., Sack, B., Wright, J.H., 2007. The U.S. Treasury yield curve: 1961 to the present. Journal of Monetary Economics 54, 2291–2304. doi:10.1016/j.jmoneco.2007.06.029.

Hansen, L.P., Heaton, J.C., Li, N., 2005. Intangible risk, in: Measuring Capital in the New Economy. University of Chicago Press, pp. 111–149. doi:10.7208/chicago/9780226116174.003.0005.

Haugen, R.A., Baker, N.L., 1996. Commonality in the determinants of expected stock returns. Journal of Financial Economics 41, 401–439. doi:10.1016/0304-405X(95)00868-F.

Hou, K., Xue, C., Zhang, L., 2015. Digesting anomalies: An investment approach. Review of Financial Studies 28, 650–705. doi:10.1093/rfs/hhu068.

Jensen, T.I., Kelly, B.T., Pedersen, L.H., 2021. Is there a replication crisis in finance? SSRN Electronic Journal doi:10.2139/ssrn.3774514.

Kogan, L., Papanikolaou, D., Seru, A., Stoffman, N., 2017. Technological innovation, resource allocation, and growth. The Quarterly Journal of Economics 132, 665–712. doi:10.1093/qje/qjw040.

Kung, H., Schmid, L., 2015. Innovation, growth, and asset prices. The Journal of Finance 70, 1001–1037. doi:10.1111/jofi.12241.

Lin, X., 2011. Endogenous technological progress and the cross-section of stock returns. Journal of Financial Economics doi:10.1016/j.jfineco.2011.08.013.

Ludvigson, S.C., Ng, S., 2009. Macro Factors in Bond Risk Premia. Review of Financial Studies 22, 5027–5067. doi:10.1093/rfs/hhp081.

Novy-Marx, R., 2013. The other side of value: The gross profitability premium. Journal of Financial Economics 108, 1–28. doi:10.1016/j.jfineco.2013.01.003.

Ortu, F., Tamoni, A., Tebaldi, C., 2013. Long-run risk and the persistence of consumption shocks. Review of Financial Studies 26, 2876–2915. doi:10.1093/rfs/hht038.

Rajan, R.G., Zingales, L., 1995. What Do We Know about Capital Structure? Some Evidence from International Data. The Journal of Finance 50, 1421–1460. doi:10.1111/j.1540-6261.1995.tb05184.x.